Characterization of the developmental landscape of murine RORγt+ iNKT cells

Jihène Klibi, Shamin Li, Ludivine Amable, Claudine Joseph, Stéphane Brunet, Marc Delord, Véronique Parietti, Jean Jaubert, Julien Marie, Saoussen Karray, et al.

HAL Id: hal-02401536
https://hal.archives-ouvertes.fr/hal-02401536

Submitted on 17 Jun 2020

Characterization of the developmental landscape of murine RORγt^{+} iNKT cells

Jihene Klibi[1,2], Shamin Li[1,2], Ludivine Amable[1,2], Claudine Joseph[1,2], Stéphane Brunet[1,2], Marc Delord[23], Veronique Parietti[2,4], Jean Jaubert[5], Julien Marie[6], Saoussen Karray[1,2], Gerard Eberl[7,8], Bruno Lucas[9], Antoine Toubert[1,2] and Kamel Benlagha[1,2]   AQ1

[1]INSERM, UMR-1160, Institut Universitaire d'Hématologie, 75010, Paris, France
[2]Université Paris Diderot, Sorbonne Paris Cité, 75010, Paris, France.
[3]Plateforme de Bioinformatique et Biostatistique, Institut Universitaire d'Hématologie, Université Paris Diderot, Sorbonne Paris Cité, 75010, Paris, France.
[4]Département d'Expérimentation Animale, Institut Universitaire d'Hématologie, 75010, Paris, France
[5]Mouse Genetics Unit, Institut Pasteur, 75015, Paris, France.
[6]Department of Immunology, Virology and Inflammation, Cancer Research Center of Lyon UMR INSERM1052, CNRS 5286, Centre Léon Bérard Hospital, Université de Lyon, Equipe labellisée LIGUE, 69008, Lyon, France.
[7]Microenvironment &Immunity Unit, Institut Pasteur, 75015, Paris, France,
[8]INSERM U1224, 75015, Paris, France.
[7]Institut Cochin, Centre National de la Recherche Scientifique UMR8104, INSERM U1016, Université Paris Descartes, 75014 Paris, France
AQ2

Corresponding author: kamel Benlagha**; kamel.benlagha@inserm.fr**; Inserm U1160, 1 Ave Claude Vellefaux, 75010 Paris, France; Researcher ID : I-5035-2016**.**

ABSTRACT

Invariant natural killer T cells (iNKT) expressing the retinoic acid receptor-related orphan receptor γt (RORγt) and producing IL-17 represent a minor subset of CD1d-restricted iNKT cells (iNKT17) in C57BL/6J (B6) mice. We aimed in this study to define the reasons for their low distribution and the sequence of events accompanying their normal thymic development. We found that RORγt$^+$ iNKT cells have higher proliferation potential and a greater propensity to apoptosis than RORγt$^-$ iNKT cells. These cells do not likely reside in the thymus indicating that thymus emigration, and higher apoptosis potential, could contribute to RORγt$^+$ iNKT cell reduced thymic distribution. Ontogeny studies suggest that mature HSA^{low} RORγt$^+$ iNKT cells might develop through developmental stages defined by a differential expression of CCR6 and CD138 during which RORγt expression and IL-17 production capabilities are progressively acquired. Finally, we found that RORγt$^+$ iNKT cells perceive a strong TCR signal that could contribute to their entry into a specific "Th17 like" developmental program influencing their survival and migration. Overall, our study proposes a hypothetical thymic developmental sequence for iNKT17 cells, which could be of great use to study molecular mechanisms regulating this developmental program.

INTRODUCTION

Mouse invariant Natural Killer T (iNKT) cells are a subset of T lymphocytes expressing a semi-invariant TCR composed by a Vα14-Jα18 chain, associated mostly with Vβ8, 7 or 2 chains, and playing an important role in innate and adaptive immune system. Unlike conventional T cells, iNKT cells do not recognize peptide antigens presented by classical MHC-I or II molecules, but glycolipid antigens presented by non-polymorphic CD1d molecule. Upon activation, iNKT cells can rapidly produce a large range of cytokines that confer them a crucial position in pathologies and regulation of immune responses (1).

iNKT cells, uniformly stained by CD1d-αGalcer tetramers, are positively selected upon recognition of CD1d expressed on cortical AQ4 (double positive) DP thymocytes loaded with glycolipids. The earliest iNKT cell precursors detected are iNKT cells at the HSA^{high} stage called stage 0. These cells have a Vβ8 bias, are non-dividing, do not express CD44, are mainly CD4+, and express CD69 reflecting the signal perceived at positive selection (2). HSA^{high} iNKT cells give rise to HSA^{low} cells that progress through three different stages. The first two stages are characterized respectively by CD44$^-$NK1.1$^-$ and CD44$^+$NK1.1$^-$ expression. Cells from both stages are receptive to IL-7 and undergo a massive expansion. The second stage iNKT cells then acquire NK cells features including NK1.1 expression in the thymus or after migration to periphery. They give rise to thymic and peripheral stage 3 iNKT cells, the former remaining thymic resident (3). Stage 3 iNKT cells produce mainly IFN-γ and their generation is under control of T-bet and IL-15 (3). A new developmental model for iNKT cells has been described recently (4). It distinguishes three iNKT cell subsets called iNKT1, iNKT2 and iNKT17, based on the expression of T-bet, PLZF and RORγt transcription factors. These subpopulations are reminiscent to those of the T helper cell lineage, and produce Th1, Th2 and Th17-like cytokines, respectively (4).

We and others contributed to the description of IL-17-producing iNKT cells lacking NK1.1 expression and mainly located in lungs, peripheral lymph nodes (PLNs), and skin (5,6). These cells express the transcription factor RORγt, and markers related to the Th17 lineage such as IL-1R, CCR6, CD103, and CD138 and have been described to be involved in inflammation, bacterial infection and autoimmunity (6-10). AQ5 The developmental stages leading to RORγt$^+$ iNKT cells, also called iNKT17, have been reported by Michel et al (11). iNKT17 cells are mainly observed at stage 2 CD44^{high} cells and pass through a CD44^{low} stage. Most HSA^{high} stage 0 iNKT cells are RORγt$^+$. The authors proposed a model where a minor population of these cells remains RORγt$^+$ to give rise to IL-17-producing iNKT cells, while the major part lose RORγt$^+$ expression and differentiate into IFN-γ and IL-4-producing iNKT cells (11).

While conventional iNKT (iNKT1) cell developmental stages are well defined, developmental and maturation sequence of RORγt$^+$iNKT cells is still unclear. In addition, the distribution of RORγt$^+$ iNKT cells in the thymus is minor compared to RORγt$^-$ iNKT cells. We aimed in this study to understand the developmental stages of these iNKT17 cells and the factors responsible for their distinct partition. We found that high apoptotic level of RORγt$^+$ iNKT cells and their emigration properties could account for their minor distribution in the thymus. We also show that RORγt$^+$ iNKT cells progress during development through defined stages and acquire progressively functional and phenotypic feature that characterize mature iNKT17 cells. We propose that their entry into a "Th17 like" program could be driven in part by a distinct signal perceived by their TCR.

MATERIAL AND METHODS

Mice

C57BL/6J (B6) and BALB/c mice were purchased from Janvier. FasL KO and *Rorc(γt)-GfpTG* mice on B6 background (B6-ROR*gfp*Tg) were described elsewhere (12,13). *Rorc(γt)-GfpTG* mice on BALB/c background (BALB/c-ROR*gfp*Tg) were generated in our laboratory by backcrossing *Rorc(γt)-GfpTG* with BALB/c mice. All mice were maintained under specific pathogen-free conditions, and experiments were performed in accordance with the Institutional Animal Care and Use Guidelines. The study was approved by the ethics committee "Comité d'Ethique Paris-Nord; C2EA-121", affiliated to the "Comité National de réflexion Ethique en Expérimentation Animale (CNREEA) et au Ministère de l'Enseignement Supérieur et de la Recherche".

Lymphocyte isolation, stimulation, and expansion

Cell suspensions from thymus or PLNs were prepared and stimulated with PMA/Ionomycin or IL-1/IL-23 as previously described (6,7). Thirty million thymocytes were incubated 5 days with IL-7 (20ng/ml; Peprotech). Cell sorting of iNKT cell subsets was performed with a FACSAria III (BD Biosciences).

5-Bromo-2′-deoxyuridine (BrdU) labeling of cells

Drinking water containing 1 mg/ml BrdU (Sigma-Aldrich, St. Louis, MO) was administered for 2 wk, with fresh water preparations made every day. BrdU-positive cells were detected with the BrdU Flow kit (BD PharMingen) according to the manufacturer's instructions.

Antibodies and flow cytometry AQ6

Before cell-surface staining, surface Fc receptors were saturated by incubation with CD16/CD32 (2.4G2) antibody from eBioscience for 15 minutes on ice. The following

5

antibodies were used : FITC, PE-Cy7, Pacific Blue and BV510 HSA (M1/69) from BioLegend; BV421 RORγt (Q31-378) BD Biosciences; PerCP-eFluor 710 RORγt (B2D) from eBioscience; PE, PerCP-Cy5.5, and FITC CD4 (RM4-5) from BD Biosciences; PE-Cy7, APC, and APC eF780 CD4 (RM4-5) from eBioscience; AF700 CD4 (RM4-5), and Pacific Blue CD4 (GK1.5) from BioLegend; Alexa Fluor 647 CCR6 (140706) from BD Biosciences and PE CCR6 (140706) from R&D Systems; AF488 CD138 (281-2) from R&D Systems, PE CD138 (281-2) from BD Biosciences, and PE-Cy7 CD138 (281-2) from BioLegend; FITC Ki-67 (SolA15) from eBioscience; FITC Annexin V from BD Biosciences and BV421 Annexin V from eBiosciences; BV510 and PerCP-Cy5.5 B220 (RA3-6B2) from BD Biosciences; PE Bcl-2(3F11) from BD Biosciences; PE IL-17a (TC11-18H10) from BioLegend and PerCP-eFluor 710 IL-17a (eBIO17B7) from eBioscience, AF700 CD44 (IM7) from BD Biosciences and BUV737 CD44 (IM7) from BioLegend; FITC and PE Vβ8, FITC CD5 (53-7.3), and FITC CD69 (H1.2F3) from BD Biosciences; APC TCR (H59-597) from eBioscience, PE PLZF (R17-809) from BioLegend. 7-aminoactinomycin D (7-AAD) was purchased from eBioscience. CD1d-α-GalCer or -PBS57 tetramers were produced with streptavidin-APC, -PE or -BV421 (BD Biosciences). The antibodies used for Nrp-1 staining were polyclonal goat anti-mouse/rat Nrp-1 (AF566; R&D Systems) and FITC donkey anti-goat IgG (F0109, R&D Systems). For intranuclear staining, cells were fixed and permeabilized using the Foxp3 staining kit (eBioscience). Intracellular cytokine staining was performed as described previously (6,7). The annexin V staining kit (BD Biosciences) was used in agreement with the recommended protocol. Flow cytometry was performed using a 4-laser Fortessa cytometer (BD Biosciences) and analyzed using FACSDiva software v8 (BD Biosciences) and FlowJo software v8.

Microarray

RNA was extracted from FACS-sorted IL-7-expanded Tet^+IL-1R^+ ($ROR\gamma t^+$) and Tet^+IL-1R^- ($ROR\gamma t^-$) thymocytes with TRIzol reagent (Invitrogen) followed by column purification using RNeasy mini Kit (QIAGEN). RNA samples were hybridized on MoGene2.0.st chips (Affymetrix). Raw chip data preprocessing and quantile-normalization were performed using RMA. Gene level data were then expressed on the log2 scale and annotated using Affymetrix MoGene2.0.st library files. Metabolic pathway analysis was performed using the Gene Set Enrichment Analysis (GSEA)(14). AQ7. Data were obtained from whole genome microarray datasets under GEO accession number GSE139084

Immunofluorescence and morphometric analysis

Sorted fresh tet+CD138+ and tet+CD138- iNKT cells were sedimented on polylysin-coated coverslips and fixed in "Cytoskeleton Buffer" (10mM MES pH 6.1 138mM KCl 3mM MgCl 2mM EGTA) containing 0,1 % Glutaraldehyde (Sigma-Aldrich). Microtubules were stained using an anti-tubulin antibody (AbD Serotec). Actin microfilaments and chromatin were labelled respectively with AF488-coupled phalloidin (Abcam) and DAPI (Sigma-Aldrich). Images were taken using an Olympus BX61 epifluorescence microscope and 100X UplanApo 1.4 olympus objective. Z series were acquired using a 0,4μm step. Image analysis was performed using Fiji software (National Institute of Health). Data were processed and statistical analyses were performed using Excel (Microsoft) and Prism (GraphPad Software, inc) softwares.

Statistical analysis

Statistical tests were performed using the two sided non-parametric Mann-Whitney U test using Prism 6.05 (GraphPad). A *p* value <0.05 was considered significant.

RESULTS

Low distribution of thymic RORγt⁺ iNKT cells despite higher proliferation

We used in this study B6-ROR*gfp*Tg mice to track IL-17-producing RORγt⁺ iNKT (iNKT17) cells based on their expression of GFP. This allows avoiding intracellular nuclear staining to identify iNKT17 cells based on RORγt expression. These mice will be used through the study unless otherwise stated. RORγt (GFP) will indicate in figures that RORγt was identified by GFP while RORγt (ic) will indicate that RORγt is identified by intracellular staining. In previous studies, we and others showed that RORγt⁺ IL-17-producing iNKT cells in B6 mice represent a minor population in the thymus and accumulate preferentially in peripheral lymph nodes (PLNs) and skin (6,7). Analysis of iNKT17 cells in 4-wk-old B6-ROR*gfp*Tg mice confirmed these results and showed that this low distribution in the thymus is already observed in a 2-wk-old mouse, and remains as such in older mice **(Fig. 1A)**. This low distribution of RORγt⁺ iNKT cells is observed at the CD44^{low} and CD44^{high} stages of iNKT cell development **(Fig. 1B).** The low distribution of iNKT17 cells is not a result of a lower response to IL-7, a cytokine iNKT cells rely on for their thymic expansion during the early stages of their development (15), since RORγt⁺ iNKT cells proliferate *in vitro* in the presence of IL-7 with higher efficacy compared to RORγt⁻ iNKT cells, as evaluated by the increase of their absolute number compared to the start of the culture (around 160 times *vs* 14 time increase of RORγt⁺ iNKT cell numbers compared to RORγt⁻ iNKT cell numbers respectively) **(Fig. 1C).** This greater response to IL-7 could be accounted for by a higher expression of IL-7R as assessed by IL-7Rα expression **(Fig. 1D).** Gene-expression analysis showed that pathways related to DNA replication, cell cycle, and homologous recombination was highly enriched in IL-7-expanded RORγt⁺ iNKT cells, confirming a higher sensitivity of these cells to IL-7 **(Fig. 1E).** We also found that RORγt⁺ iNKT cells expand *in vivo* with a better efficiency than RORγt⁻ iNKT cells at both CD44^{low} and CD44^{high} stages, as assessed by

8

intracellular nuclear Ki-67 expression in a 4-wk-old B6 mouse (**Fig. 1F**). The higher expansion capacity of RORγt$^+$ iNKT cells is not specific to the B6 strain as we observed the same trend in BALB/c mice (**Fig. S1**).

Overall, our results indicate that neither a defect in response to IL-7 nor *in vivo* lineage expansion could account for the lower frequency and number of thymic RORγt$^+$ iNKT cells in B6 mice.

B6-ROR*gfp*Tg mice is not suitable to study HSA^{high} stage 0 iNKT cells

We next sought to characterize the earliest RORγt$^+$ iNKT cells precursors at the previously named stage 0 using B6-ROR*gfp*Tg mice as RORγt expression was not documented at this stage. Cells at this stage can be identified as binding CD1d/α-GalCer tetramer, and are HSA^{high}, CD44^{low}, NK1.1$^-$, and mainly CD4$^+$ (2). iNKT cells at stage 0 also express CD69 reflecting the signal perceived at positive selection occurring at the DP stage (2). Importantly, we have to consider the fact that DP thymocytes strongly express RORγt (16), so DP thymocytes would express GFP strongly in B6-ROR*gfp*Tg mice. As a consequence, upon positive selection of TCR^{int}CD69$^+$ thymocytes from the preselected DP TCR^{low} pool, RORγt expression is downregulated in these TCR^{int}CD69$^+$ selected cells but the GFP protein remains, since the half-life of GFP protein is relatively long (**Sup.S2**). Based on that, we expect that GFP-expressing HSA^{high} Tet$^+$ stage 0 iNKT cells will not have the expected RORγt expression**.** In fact, we found that while around 40 to 45% of iNKT cells detected in B6-ROR*gfp*Tg mice are RORγt$^+$, based on GFP expression, rare iNKT cells expressing nuclear RORγt at the HSA^{high} stage are detected by intracellular staining in B6 mice (0.5 to 2% of HSA^{high} iNKT cells) (**Sup.S2**). An unambiguous characterization of these cells was not possible due to their rarity. These results indicate that B6-ROR*gfp*Tg mice AQ8 do not allow the study early post positively selected HSA^{high} iNKT cells.

RORγt⁺ iNKT cells experience apoptosis during development

We next hypothesized that the low RORγt$^+$ iNKT cell numbers in B6 mice could be due to a reduced survival caused by a higher rate of apoptosis. We found that thymic RORγt$^+$ iNKT cells show a greater apoptotic cell proportion compared to RORγt$^-$ iNKT cells (on average 25% vs 5%) **(Fig. 2A).** Interestingly, apoptosis occurs mostly at the early CD44^{low} stage **(Fig. 2A).** In fact, annexin V positive cells represent around 40% of CD44^{low} RORγt$^+$ iNKT cells while they represent around 5% of RORγt$^+$ CD44^{high} iNKT cells**.** To examine the molecular mechanism responsible of the higher apoptosis of RORγt$^+$ iNKT cells, we first tested the potential role of the extrinsic apoptosis pathway by analyzing FasL KO mice and found that thymic RORγt$^+$ frequency and absolute numbers in these mice are similar to littermate control B6 mice **(Fig. 2B).** Consistent with this result, the frequency of Annexin V positive cells among thymic CD44^{low} RORγt$^+$ iNKT was comparable in FasL KO mice and in B6 control mice **(Fig. 2B).** Second, we tested a potential role of the intrinsic apoptotic pathway by analyzing intracellular nuclear Bcl-2 expression in B6 mice and found that RORγt$^+$ iNKT cells express low levels of Bcl-2 compared to RORγt$^-$ iNKT cells, at both CD44^{low} and CD44^{high} stage **(Fig. 2C).** These results are in accordance with published transcriptome analysis indicating a lower Bcl-2 expression in RORγt$^+$ iNKT (17). Interestingly, IL-7 signaling did not reverse the apoptosis transcriptional profiles of RORγt$^+$ iNKT cells as we detect no upregulation of Bcl-2 in the presence of IL-7, but a greater expression of the intrinsic Bcl2-dependent pro-apoptotic genes in this subset **(Fig. 2D).** In addition, Gene-set–enrichment analysis indicated a specific enrichment of genes related to the apoptotic P53 signaling pathway in RORγt$^+$ iNKT cells **(Fig. 2E).** Interestingly, RORγt$^+$ iNKT from BALB/c-ROR*gfp*Tg mice do not show a higher apoptosis potential compared to RORγt$^-$ iNKT cells indicating that this feature is strain specific **(Fig. S3**).

These results show that thymic RORγt$^+$ iNKT cells in B6 mice experience a greater apoptosis potential than RORγt$^-$ iNKT cells that could explain in part their reduced number.

Differential expression of CD138 and CCR6 during thymic RORγt$^+$ iNKT cell development

In PLNs of adult mice, we showed in a previous study that mature RORγt$^+$ iNKT cells express IL-1R, CCR6, and CD103, and produce IL-17 (6). In addition, a more recent study showed that RORγt$^+$ iNKT cells express CD138 (10). We performed ontogeny studies to assess how these phenotypic and functional features develop. Single staining analysis showed a dynamic change in the expression of CD138 and CCR6 in the thymus, where we observed a progressive acquisition of these markers by RORγt$^+$ iNKT cells **(Fig. 3A).** Concomitant analysis of CD138 and CCR6 expression in the thymus suggest that RORγt$^+$ iNKT cells likely progress through 3 developmental stages during their development starting from a CD138$^-$ CCR6$^-$ stage, an intermediate CD138$^+$ CCR6$^-$ stage, and a CD138$^+$ CCR6$^+$ end stage, that we named respectively stage 1', 2', and 3' **(Fig. 3B).** Analysis of CD138 and CCR6 expression in thymic RORγt$^+$ iNKT cells at the CD44^{low} stage showed mainly early stage 1'cells **(Fig. 3C)**. At the CD44^{high} development stage, all stages from 1' to 3' are observed **(Fig. 3C)**. This potential developmental sequence is also observed in PLNs, suggesting that maturation of RORγt$^+$ iNKT cells could take place in the periphery **(Fig. S4A, and B).** In support for the AQ9 developmental sequence proposed is the progressive RORγt expression acquisition paralleling with increased IL-17 production capability from early stage 1', where IL-17 is barely detected, to stage 3', where the highest IL-17 production is observed **(Fig. 3D, and E).** Also, a progressive reduction in the propensity to apoptosis is observed along this sequence **(Fig. S5)**. An additional support for the proposed hypothetic sequence is the progressive decrease in the proliferation of RORγt$^+$ iNKT cells from stage 1' to 3' **(Fig. 3F)**. Since high

proliferation characterizes early stages of development, stage 1', composing most of the CD44^{low} stage, would represent the earliest stage of development, while stage 3', with the lowest proliferation status, a final developmental stage. Progression from stage 1' to 3' in PLNs is also characterized by increased expression of RORγt and IL-17 production capacity **(Fig. S4C, and D)**.

Overall ontogeny studies suggested that developing RORγt$^+$ iNKT cells acquired progressively phenotypic and functional features leading to fully mature CCR6$^+$CD138$^+$RORγt$^+$ iNKT cells in the thymus and PLNs. The proposed developmental sequence of event is depicted in **Figure S6.** The proposed model is hypothetical and experiment demonstrating precursor-product relationships are warranted to validate this proposed model.

RORγt$^+$ iNKT cells are likely not to accumulate in the thymus

To further characterize RORγt$^+$ iNKT cells, we investigated their morphology by immunofluorescence analysis on sorted RORγt$^+$ iNKT from B6 mice, identified as CD138$^+$ iNKT cells, to allow the usage of FITC-labeled probes that would have interfered with GFP if we were to use B6-ROR*gfp*Tg mice. We found that RORγt$^+$ iNKT cells were considerably larger than RORγt$^-$ iNKT cells (mean cell area values of 50 μm^2 and 35 μm^2 respectively (p<0,0001, Mann Whiney test) **(Fig. 4A)** and contained a more expanded cytoplasm. Finally, we found that most of these cells were elongated **(Fig. 4A)**; a morphology reported to characterize migrating cells (18-20). FACS analysis confirmed these results and showed that CD138$^+$ iNKT cells in B6 mice have higher cell size and granularity, a latter feature that might be explained by their expanded cytoplasm **(Fig. 4B)**. FACS analysis of RORγt$^+$ iNKT identified as of GFP$^+$ cells in B6-ROR*gfp*Tg mice showed the same results (**Fig. 1A, and data not shown**).

To further document the migration status of RORγt$^+$ iNKT cells, we analyzed neuropilin-1 expression, the non-expression of which correlates with thymic residency (21), and found that the majority of RORγt$^+$ iNKT cells express neuropilin-1 (**Fig. 4C, left panel**). This expression is stable over time (**Fig. 4C, middle panel**) and is similar in CCR6$^+$ and CCR6$^-$ expressing cells (**Fig. 4C, right panel**), suggesting that both CCR6$^+$ and CCR6$^-$ RORγt$^+$ iNKT cells might leave the thymus and not accumulate in this organ. In support for this notion, CCR6$^-$RORγt$^+$ iNKT cells are observed in PLNs concomitantly with CCR6$^+$RORγt$^+$ iNKT cells at all ages tested (**Fig. S4B**). In order to demonstrate that RORγt$^+$ iNKT cells do leave the thymus, we provided B6 mice with BrdU-supplemented water for 2 wk. BrdU positive cells will be detected by intracellular nuclear staining. As shown in **Figure 4D**, under continuous BrdU exposure for 2 wk, RORγt$^+$ iNKT cells exhibited a markedly increased frequency of BrdU$^+$ cells compared to RORγt$^-$ iNKT cells (30% vs 40%, on average) confirming the higher proliferation of RORγt$^+$ iNKT cells observed (**see Fig. 1C, and F**). After 2 wk of chase, the frequency of BrdU$^+$ cells among RORγt$^+$ iNKT cells decreased 4-fold (from 40 to 10% on average) indicating that the majority RORγt$^+$ iNKT cells are likely non-thymus resident. The loss of BrdU staining could also be due to proliferation of RORγt$^+$ iNKT cells within the tissue. Even if it was the case, we believe this occurs concomitantly with emigration since RORγt$^+$ iNKT cell number do not increase in old mice as illustrated in **figure 1A**. As a positive control for our BrdU experiment, and contrary to what observed for RORγt$^+$ iNKT cells, we found that the frequency of BrdU$^+$ cells among RORγt$^-$ iNKT cells remain unchanged, indicating that these cells are thymic resident like described previously (3,22).

Overall these results suggest that thymic RORγt$^+$ iNKT cells expressing neuropilin-1 do not likely reside in the thymus and this might contribute to their reduced number in this organ.

RORγt⁺ iNKT cells perceive a distinct TCR signal during maturation

Published results indicated that iNKT cells perceive a stronger stimulus than conventional T cells upon selection in the thymus (23). With the notion that TCR signal strength might provide information reflecting their survival properties and fate, we monitored the expression of CD5, a marker known to transduce TCR signal strength perceived at the positive selection stage. We performed this analysis in B6 mice since we have to perform intracellular nuclear staining to define iNKT cell subsets based on their expression of specific transcription factors. Also, we used 2-wk-old young mice because the CD44^{low} maturation stage is abundant in these mice compared to older mice. Analysis of this CD44^{low} maturation stage is important since we detected at this stage a high propensity to apoptosis of RORγt⁺ iNKT cells (**see figure 3A**). As shown in **figure 5A**, we found a differential surface expression level of CD5 in different iNKT cell subsets with an expression in NKT2 cells (PLZF^{high}RORγt⁻T-bet⁻) > NKT17 cells (PLZF^{int}RORγt⁺) > NKT1 cells (PLZF^{int}RORγt⁺T-bet⁺), in accordance with previous studies (24). We observed the same hierarchy of expression level of CD5 at the CD44^{high} stage of iNKT cell development. However, at the CD44^{low} stage, we found that iNKT17 cells have the highest level of CD5 expression. Based on these results, we decided to compare the apoptosis rate of the different subsets by evaluating annexin V expression. As shown in **figure 5B**, we confirmed the high apoptosis rate of iNKT17 cells at the CD44^{low} stage, and not at the CD44^{high} stage, as observed in B6-ROR*gfp*Tg mice **(see figure 3A).** In addition we found that iNKT2 cells have a high rate of apoptosis, quite similar to the one observed for iNKT17 cells at the same CD44^{low} stage. At the CD44^{high} stage, only iNKT2 cells keep a high rate of apoptosis but twice lower than the one observed at the CD44^{low} stage.

Overall, these results indicate that developing RORγt$^+$ iNKT cells perceive during their maturation a differential signal that could contribute their entry into a specific developmental program.

DISCUSSION

We aimed in this study to characterize the genesis of RORγt^{+} iNKT cells and understand why they represent a minor subset of iNKT cells in C57BL/6J mice by using B6-ROR*gfp*Tg mice where we can track IL-17-producing RORγt[+] iNKT (iNKT17) cells based on their expression of GFP. We show that RORγt^{+} iNKT cells might follow a developmental sequence based on differential expression of CD138 and CCR6 accompanied by a propensity to apoptosis and incapacity to reside in the thymus. We also found that a strong TCR signal could contribute their entry into a specific developmental program.

We wanted to inquire in this study whether the reduced distribution of RORγt^{+} iNKT cells could be at the positive selection level. To address this question we wanted to analyze these cells at the HSA[high] stage 0 of development in B6-ROR*gfp*Tg mice. However, such analysis could not be performed as we found that GFP expression do not reflect RORγt expression. In fact, while half of HSA^{high} iNKT cells detected in B6-ROR*gfp*Tg mice are RORγt[+] based on GFP expression, RORγt^{+} iNKT cells detected by intracellular nuclear staining at this stage in B6 mice are very rare and barely detectable even after enrichment strategies (less than 2% of HSA^{high} iNKT cells). Thus due to the relatively long half-life of GFP, B6-ROR*gfp*Tg mice do not constitute a suitable tool to study early post positively selected HSA^{high} iNKT cells.

Previously, we showed in B6 mice that HSA[high] stage 0 iNKT cells are resting with a small size and granulometry compared to proliferating mature iNKT cells (2). The cells express CD69, indicator of a post-positive selection stage, and have already a Vβ8 bias. They are CD44^{low}, and all the cells express CD4 early after birth (2). In a published study by Mitchell et al, early HSA^{high} iNKT cells expressing CD8 (supposed to be DP) were detected without enrichment strategy and all these cells were shown to express RORγt (11). The proposed model based on this study suggests that some DP HSA[high] RORγt[+] precursors keep RORγt

16

expression to give rise to HSA^{low} RORγt$^+$ iNKT cells. iNKT cells that down regulate RORγt$^+$ enter a distinct developmental program. An alternative model could be that RORγt$^+$ iNKT cells are the product of a maturation program where RORγt is acquired after positive selection. In this model, positively selected HSA^{high} RORγt$^+$ iNKT cells precursors lose expression of RORγt and re-express RORγt when entering a "Th17 like" like program. A study by the Bevan's group showing that down-regulation of RORγt expression is essential for the maturation of DP thymocytes into SP thymocytes would support this model (25). In addition, a more recent study distinguished between the function of RORγt in Th17 differentiation and its function in thymocyte development and revealed distinct mechanism for these two RORγt-regulated processes (26).

Published results indicated that RORγt$^+$ iNKT rely completely on IL-7 for their development and indicated that their preferential response to IL-7 does not reflect enhanced signaling through STAT proteins, but instead is modulated via the PI3K/AKT/mTOR signaling pathway (27). In T cells, the PI3K pathway is primarily activated after engagement of TCR in conjunction with co-stimulatory receptors (28). Our analysis of receptor expression reflecting the TCR signal strength perceived by developing RORγt$^+$ iNKT cells, assessed by CD5 expression, show a strong TCR signal perceived by RORγt$^+$ iNKT cells indicating that a specific TCR signal in conjunction with IL-7 could contribute to the entry of iNKT cell precursors into a "Th17-like" program of differentiation. Our results are in agreement with recent studies showing that differential TCR signaling could impact thymic differentiation of iNKT cell subsets (24,29).

Syndecan-1 (SDC-1; CD138) a heparan sulfate proteoglycans expressed in epithelial cells (30,31) was recently shown to be a surface marker of iNKT17 cells (10). Here we found that

early CD44^{low} RORγt$^+$ iNKT do not express CD138 and CCR6. The CD138$^-$CCR6$^-$ RORγt$^+$ iNKT cells might represent the earliest developmental stage that we called stage 1' at the CD44^{low} stage. These CD138$^-$CCR6$^-$ RORγt$^+$ iNKT are supposed to express CD44 and give rise to CD44^{high}CD138$^-$CCR6$^-$ RORγt$^+$ iNKT cells (called stage1' occurring at the CD44^{high} stage). The cells likely express CD138 to give rise to CCR6$^-$CD138$^+$ cells (stage 2'). Finally, CD138$^+$CCR6$^+$ cells could represent the final stage of iNKT17 development (stage 3'). Along this hypothetical sequence, these cells progressively became less prone to apoptosis, cease division, express RORγt, and acquire the capacity to produce IL-17. Different results in this study, including BrdU incorporation experiment, concur to the fact that RORγt$^+$ iNKT cells are not thymic resident. In addition, ontogeny studies showed an increased frequency of CD138$^+$CCR6$^+$ iNKT cells in PLNs indicating that a maturation of RORγt$^+$ iNKT cells could occur in the periphery contributing to the pool of mature iNKT cells in PLNs. A proposed model for the thymic and peripheral development of RORγt$^+$ iNKT cells is shown in **Figure S6.** This model is hypothetical because missing experiments demonstrating precursor product relationship.

Several studies have compared iNKT17 subset distribution in various inbred strains (4,32,33) and pointed out an increased frequency and absolute number of these cells in BALB/c and NOD mice. Our results indicate that RORγt$^+$ iNKT thymocytes from BALB/c-ROR*gfp*Tg mice have higher expansion efficiency than RORγt$^-$ iNKT thymocytes. However, this feature is also observed in their homologs in B6-ROR*gfp*Tg mice. This indicates that establishment of a higher distribution RORγt$^+$ iNKT cells in BALB/c mice is not a result of a specific higher expansion potential. However, we found that RORγt$^+$ iNKT cells in BALB/c-ROR*gfp*Tg mice, contrary to B6-ROR*gfp*Tg mice, have a reduced susceptibility to apoptosis, which could contribute to their higher proportion compared to their homologs in B6 mice. The high

susceptibility to apoptosis we observed for developing RORγt^{+} iNKT cells in B6 mice was also reported for developing DP[low] CD8αα[+] IEL (34). Importantly, these cells were shown to perceive an elevated T cell signaling promoting their so called "agonist selection". A recent study showed a higher expression of Egr2 transcript in iNKT17 cells from B6 compared to BALB/c mice suggesting that these cells perceive a stronger TCR signal during development; and this might explain their propensity to apoptosis (29). The same study found that the signal reflecting S1P1 mRNA expression was close to background level in BALB/c but not B6 iNKT17 cells (29). They also showed that iNKT17 recent thymic emigrant (RTE) cells (that are very rare) are more frequent in B6 than BALB/c mice. This indicates that inefficient emigration of iNKT17 cells in BALB/c mice, in addition to their non-propensity to apoptosis, could provide a potential explanation why iNKT17 cells in BALB/c mice are more frequent as compared with B6 mice. Factors like β-catenin regulating iNKT2 cells, which are the major iNKT subset in BALB/c mice, could contribute at the same time to iNKT17 cell establishment in this strain (35). In NOD mice, a recent study reveals that their excessive iNKT17 cell frequency correlates with miRNA-133B-mediated defective Th-POK expression (33), described to repress iNKT17 cell development (36). All these observations indicate that in addition to the arguments we provided to explain the differences in thymic RORγt[+] iNKT cell distribution, there could be strain-specific regulation factors that could influence iNKT17 cell distribution.

In conclusion, our study provides a phenotypic and functional thymic and peripheral hypothetical sequence of development of RORγt^{+} iNKT cells in C57BL/6J mice and explains in part the possible origin of their reduced frequency and numbers. This study thus lays the ground for future studies aiming at addressing the molecular mechanisms and checkpoints regulating this developmental program.

REFERENCES

1   Bendelac, A., Savage, P. B., and Teyton, L. 2007. The biology of NKT cells. *Annu Rev Immunol* 25:297.

2   Benlagha, K., Wei, D. G., Veiga, J., Teyton, L., and Bendelac, A. 2005. Characterization of the early stages of thymic NKT cell development. *J Exp Med* 202:485.

3   Benlagha, K., Kyin, T., Beavis, A., Teyton, L., and Bendelac, A. 2002. A thymic precursor to the NK T cell lineage. *Science* 296:553.

4   Lee, Y. J., Holzapfel, K. L., Zhu, J., Jameson, S. C., and Hogquist, K. A. 2013. Steady-state production of IL-4 modulates immunity in mouse strains and is determined by lineage diversity of iNKT cells. *Nat Immunol* 14:1146.

5   Michel, M. L., Keller, A. C., Paget, C., Fujio, M., Trottein, F., Savage, P. B., Wong, C. H., Schneider, E., Dy, M., and Leite-de-Moraes, M. C. 2007. Identification of an IL-17-producing NK1.1(neg) iNKT cell population involved in airway neutrophilia. *J Exp Med* 204:995.

6   Doisne, J. M., Becourt, C., Amniai, L., Duarte, N., Le Luduec, J. B., Eberl, G., and Benlagha, K. 2009. Skin and peripheral lymph node invariant NKT cells are mainly retinoic acid receptor-related orphan receptor (gamma)t+ and respond preferentially under inflammatory conditions. *J Immunol* 183:2142.

7   Doisne, J. M., Soulard, V., Becourt, C., Amniai, L., Henrot, P., Havenar-Daughton, C., Blanchet, C., Zitvogel, L., Ryffel, B., Cavaillon, J. M., Marie, J. C., Couillin, I., and Benlagha, K. 2011. Cutting edge: crucial role of IL-1 and IL-23 in the innate IL-17 response of peripheral lymph node NK1.1- invariant NKT cells to bacteria. *J Immunol* 186:662.

8   Yoshiga, Y., Goto, D., Segawa, S., Ohnishi, Y., Matsumoto, I., Ito, S., Tsutsumi, A., Taniguchi, M., and Sumida, T. 2008. Invariant NKT cells produce IL-17 through IL-23-dependent and -independent pathways with potential modulation of Th17 response in collagen-induced arthritis. *Int J Mol Med* 22:369.

9   Pichavant, M., Goya, S., Meyer, E. H., Johnston, R. A., Kim, H. Y., Matangkasombut, P., Zhu, M., Iwakura, Y., Savage, P. B., DeKruyff, R. H., Shore, S. A., and Umetsu, D. T. 2008. Ozone exposure in a mouse model induces airway hyperreactivity that requires the presence of natural killer T cells and IL-17. *J Exp Med* 205:385.

10   Dai, H., Rahman, A., Saxena, A., Jaiswal, A. K., Mohamood, A., Ramirez, L., Noel, S., Rabb, H., Jie, C., and Hamad, A. R. 2015. Syndecan-1 identifies and controls the frequency of IL-17-producing naive natural killer T (NKT17) cells in mice. *Eur J Immunol* 45:3045.

11   Michel, M. L., Mendes-da-Cruz, D., Keller, A. C., Lochner, M., Schneider, E., Dy, M., Eberl, G., and Leite-de-Moraes, M. C. 2008. Critical role of ROR-gammat in a new thymic pathway leading to IL-17-producing invariant NKT cell differentiation. *Proc Natl Acad Sci U S A* 105:19845.

12   Karray, S., Kress, C., Cuvellier, S., Hue-Beauvais, C., Damotte, D., Babinet, C., and Levi-Strauss, M. 2004. Complete Loss of Fas Ligand Gene Causes Massive Lymphoproliferation and Early Death, Indicating a Residual Activity of gld Allele. *The Journal of Immunology* 172:2118.

13   Lochner, M., Peduto, L., Cherrier, M., Sawa, S., Langa, F., Varona, R., Riethmacher, D., Si-Tahar, M., Di Santo, J. P., and Eberl, G. 2008. In vivo equilibrium of

proinflammatory IL-17+ and regulatory IL-10+ Foxp3+ RORgamma t+ T cells. *J Exp Med* 205:1381.

14   Subramanian, A., Tamayo, P., Mootha, V. K., Mukherjee, S., Ebert, B. L., Gillette, M. A., Paulovich, A., Pomeroy, S. L., Golub, T. R., Lander, E. S., and Mesirov, J. P. 2005. Gene set enrichment analysis: a knowledge-based approach for interpreting genome-wide expression profiles. *Proc Natl Acad Sci U S A* 102:15545.

15   Matsuda, J. L., Gapin, L., Sidobre, S., Kieper, W. C., Tan, J. T., Ceredig, R., Surh, C. D., and Kronenberg, M. 2002. Homeostasis of V alpha 14i NKT cells. *Nat Immunol* 3:966.

16   Sun, Z., Unutmaz, D., Zou, Y. R., Sunshine, M. J., Pierani, A., Brenner-Morton, S., Mebius, R. E., and Littman, D. R. 2000. Requirement for RORgamma in thymocyte survival and lymphoid organ development. *Science* 288:2369.

17   Engel, I., Seumois, G., Chavez, L., Samaniego-Castruita, D., White, B., Chawla, A., Mock, D., Vijayanand, P., and Kronenberg, M. 2016. Innate-like functions of natural killer T cell subsets result from highly divergent gene programs. *Nat Immunol* 17:728.

18   Vargas, P., Barbier, L., Saez, P. J., and Piel, M. 2017. Mechanisms for fast cell migration in complex environments. *Curr Opin Cell Biol* 48:72.

19   Somersalo, K., Carpen, O., Saksela, E., Gahmberg, C. G., Nortamo, P., and Timonen, T. 1995. Activation of natural killer cell migration by leukocyte integrin-binding peptide from intracellular adhesion molecule-2 (ICAM-2). *J Biol Chem* 270:8629.

20   Virtanen, I., Ylanne, J., Vartio, T., and Saksela, E. 1991. Human natural killer cells express different integrins and spread on fibronectin. *Scand J Immunol* 33:421.

21   Milpied, P., Massot, B., Renand, A., Diem, S., Herbelin, A., Leite-de-Moraes, M., Rubio, M. T., and Hermine, O. 2011. IL-17-producing invariant NKT cells in lymphoid organs are recent thymic emigrants identified by neuropilin-1 expression. *Blood* 118:2993.

22   Berzins, S. P., McNab, F. W., Jones, C. M., Smyth, M. J., and Godfrey, D. I. 2006. Long-term retention of mature NK1.1+ NKT cells in the thymus. *J Immunol* 176:4059.

23   Moran, A. E., Holzapfel, K. L., Xing, Y., Cunningham, N. R., Maltzman, J. S., Punt, J., and Hogquist, K. A. 2011. T cell receptor signal strength in Treg and iNKT cell development demonstrated by a novel fluorescent reporter mouse. *J Exp Med* 208:1279.

24   Tuttle, K. D., Krovi, S. H., Zhang, J., Bedel, R., Harmacek, L., Peterson, L. K., Dragone, L. L., Lefferts, A., Halluszczak, C., Riemondy, K., Hesselberth, J. R., Rao, A., O'Connor, B. P., Marrack, P., Scott-Browne, J., and Gapin, L. 2018. TCR signal strength controls thymic differentiation of iNKT cell subsets. *Nat Commun* 9:2650.

25   He, Y. W., Beers, C., Deftos, M. L., Ojala, E. W., Forbush, K. A., and Bevan, M. J. 2000. Down-regulation of the orphan nuclear receptor ROR gamma t is essential for T lymphocyte maturation. *J Immunol* 164:5668.

26   He, Z., Ma, J., Wang, R., Zhang, J., Huang, Z., Wang, F., Sen, S., Rothenberg, E. V., and Sun, Z. 2017. A two-amino-acid substitution in the transcription factor RORgammat disrupts its function in TH17 differentiation but not in thymocyte development. *Nat Immunol* 18:1128.

27   Webster, K. E., Kim, H. O., Kyparissoudis, K., Corpuz, T. M., Pinget, G. V., Uldrich, A. P., Brink, R., Belz, G. T., Cho, J. H., Godfrey, D. I., and Sprent, J. 2014. IL-17-producing NKT cells depend exclusively on IL-7 for homeostasis and survival. *Mucosal Immunol* 7:1058.

28   Deane, J. A. and Fruman, D. A. 2004. Phosphoinositide 3-kinase: diverse roles in immune cell activation. *Annu Rev Immunol* 22:563.

29   Georgiev, H., Ravens, I., Benarafa, C., Forster, R., and Bernhardt, G. 2016. Distinct gene expression patterns correlate with developmental and functional traits of iNKT subsets. *Nat Commun* 7:13116.

30   Bernfield, M., Gotte, M., Park, P. W., Reizes, O., Fitzgerald, M. L., Lincecum, J., and Zako, M. 1999. Functions of cell surface heparan sulfate proteoglycans. *Annu Rev Biochem* 68:729.

31   Khotskaya, Y. B., Dai, Y., Ritchie, J. P., MacLeod, V., Yang, Y., Zinn, K., and Sanderson, R. D. 2009. Syndecan-1 is required for robust growth, vascularization, and metastasis of myeloma tumors in vivo. *J Biol Chem* 284:26085.

32   Li, S., Joseph, C., Becourt, C., Klibi, J., Luce, S., Dubois-Laforgue, D., Larger, E., Boitard, C., and Benlagha, K. 2014. Potential role of IL-17-producing iNKT cells in type 1 diabetes. *PLoS One* 9:e96151.

33   Di Pietro, C., De Giorgi, L., Cosorich, I., Sorini, C., Fedeli, M., and Falcone, M. 2016. MicroRNA-133b Regulation of Th-POK Expression and Dendritic Cell Signals Affect NKT17 Cell Differentiation in the Thymus. *J Immunol*.

34   McDonald, B. D., Bunker, J. J., Ishizuka, I. E., Jabri, B., and Bendelac, A. 2014. Elevated T cell receptor signaling identifies a thymic precursor to the TCRalphabeta(+)CD4(-)CD8beta(-) intraepithelial lymphocyte lineage. *Immunity* 41:219.

35   Berga-Bolanos, R., Sharma, A., Steinke, F. C., Pyaram, K., Kim, Y. H., Sultana, D. A., Fang, J. X., Chang, C. H., Xue, H. H., Heller, N. M., and Sen, J. M. 2015. beta-Catenin is required for the differentiation of iNKT2 and iNKT17 cells that augment IL-25-dependent lung inflammation. *BMC Immunol* 16:62.

36   Engel, I., Zhao, M., Kappes, D., Taniuchi, I., and Kronenberg, M. 2012. The transcription factor Th-POK negatively regulates Th17 differentiation in Valpha14i NKT cells. *Blood* 120:4524.

Figure legends

Figure 1. RORγt⁺iNKT cells experience a greater proliferation than RORγt⁻ iNKT cells.
A. Flow cytometry analysis of thymic RORγt⁺ iNKT cells gated on tet⁺HSA^{low} cells from 4-wk-old ROR*gfp*Tg mice on C57BL/6J (B6-ROR*gfp*Tg) background. The frequency and absolute numbers of RORγt⁺ iNKT cells are determined in the thymus at the indicated ages.
B. Representative dot plot of thymic RORγt/CD44 gated on tet⁺ cells in 3-wk-old B6-ROR*gfp*Tg mice. Histogram plots show the frequency and absolute numbers of tet⁺RORγt⁺ iNKT cells at the CD44^{high} or CD44^{low} stage.
C. Thirty millions thymocytes from 4-wk-old B6-ROR*gfp*Tg mice are cultured for 5 days in presence of IL-7. Flow cytometry analyses of RORγt⁺ among HSA^{low}tet⁺ cells before and after culture are shown. Histograms show absolute numbers of RORγt⁺ or RORγt⁻ iNKT cells before and after culture. Numbers displayed in histograms represent fold increase in cell numbers.
D. Histograms plots of IL-7Rα expression gated on thymic tet⁺RORγt⁺ or tet⁺RORγ⁻ iNKT cells from 6-wk-old B6-ROR*gfp*Tg mice. Histograms show mean fluorescence intensity (MFI) of IL-7Rα expression in the indicated subsets.
E. Gene set enrichment analysis comparing expression of KEGG pathways between thymic IL-7-expanded RORγt⁺ and RORγt⁻ iNKT subsets.
F. Proliferation of thymic iNKT cells analyzed by intracellular nuclear expression (ic) of Ki-67 by flow cytometry in 4-wk-old B6 mice. Histograms show Ki67 frequencies in the indicated subsets.
Data are from 3 to 6 experiments where 3 to 4 mice were used per experiment. Numbers in histogram plots and dot plots represent percentages. Significance is represented by an asterisk and was evaluated with non-parametric Mann-Whitney U test. A *p* value <0.05 was considered significant. Iso: isotype control. Ic: intracellular staining.

Figure 2. RORγt⁺iNKT cells experience apoptosis during their development
A. Thymic RORγt⁺ vs RORγt⁻ iNKT cells from 3 to 4-wk-old B6-ROR*gfp*Tg mice are analyzed by flow cytometry for apoptosis after Annexin V and 7-AAD staining. Histograms represent the frequency of annexin V⁺ cells in the indicated stages and subsets.
B. Flow cytometry analysis of enriched RORγt⁺ iNKT cells, detected by intracellular nuclear staining (ic), gated on tet⁺ iNKT cells in thymus of FasL KO and littermate control B6 mice. Histograms represent the frequency and absolute numbers of RORγt⁺ iNKT cells and the frequency of annexin V⁺ cells at the CD44^{low} stage of B6 and FasL KO mice.
C. Flow cytometry analysis of Bcl-2 expression gated on thymic tet⁺RORγt⁺ and tet⁺RORγt⁻ CD44^{low} or CD44^{high} iNKT cells from 4-wk-old B6 mice assessed after intracellular nuclear staining. Histograms show the frequency of Bcl-2 positive cells in the indicated subsets.
D. Heatmap of selected genes connected to the apoptosis pathway for the differential expression between thymic IL-7-expanded RORγt⁺ vs RORγt⁻ iNKT cells.
E. Gene set enrichment analysis comparing expression of KEGG pathways between thymic IL-7-expanded RORγt⁺ and RORγt⁻ iNKT cell subsets.
Data are from 4 to 6 experiments where at least 3 mice were used per experiment. Significance is represented by an asterisk and was evaluated with non-parametric Mann-Whitney U test. A *p* value <0.05 was considered significant. NS: non-significant. Numbers represent percentages of positive cells in the indicated gates. Ic: intracellular nuclear staining.

Figure 3. Ontogeny of thymic RORγt⁺ iNKT cells

A. Histograms show the frequencies of CCR6 and CD138 positive cells among thymic tet$^+$RORγt$^+$ iNKT cells from B6-ROR*gfp*Tg mice at the indicated ages.

B. Representative dot plots of CD138/CCR6 expression among thymic tet$^+$RORγt$^+$ iNKT cells from B6-ROR*gfp*Tg mice mice at 10 days, 4 wk, and 6 wk of age. 1', 2', and 3' represent potential successive developmental stages.

C. Representative dot plots of CD138/CCR6 expression among thymic tet$^+$RORγt$^+$ CD44^{low} or CD44^{high} iNKT cells from 4-wk-old B6-ROR*gfp*Tg mice. Histograms show the frequencies and absolute numbers of the indicated stages among tet$^+$RORγt$^+$CD44^{high} or CD44^{low} iNKT cells.

D. Representative histogram plots of RORγt expression among thymic tet$^+$RORγt$^+$ CD44^{low} or CD44^{high} iNKT cells from 4-wk-old B6-ROR*gfp*Tg mice. Histograms show mean fluorescence intensity (MFI) of RORγt expression at the indicated subsets among tet$^+$RORγt$^+$CD44^{high} or CD44^{low} iNKT cells.

E. Representative histogram plots of IL-17a production by thymic RORγt$^+$ iNKT cells from 6-wk-old B6-ROR*gfp*Tg mice at the indicated stages analyzed after 4h PMA/Ionomycin. Histograms show the frequencies of IL-17a positive cells among the indicated RORγt$^+$ iNKT cell stages.

F. Representative dot plots of Ki-67 expression, assessed by intracellular nuclear staining (ic), by thymic tet$^+$CD44^{high}RORγt$^+$ iNKT cells from 6-wk-old B6 mice at the indicated stages. Histograms show the frequency of Ki-67$^+$ cells at the indicated stages in 4- to 6-wk-old mice.

Data are from 4 to 6 experiments where at least 3 mice were used per experiment. Significance is represented by an asterisk and was evaluated with non-parametric Mann-Whitney U test. A *p* value <0.05 was considered significant. NS: non-significant. Numbers represent percentages. Iso: isotype control. Ic: intracellular nuclear staining.

Figure 4. RORγt$^+$iNKT are likely not thymic resident

A. Intracellular organization of thymic CD138$^+$ and CD138$^-$ iNKT cells sorted from 4- to 6-wk-old B6 mice (left panel): representative immunofluorescence images of round and elongated RORγt$^+$ iNKT (first row, cell circularity=0,769; second row, cell circularity=0.5), round RORγt$^-$ iNKT cells (third row, cell circularity=0.74). Maximum Z-stack projections of actin microfilaments (µfts), microtubules (MTs), and chromatin (DNA) are presented. In the merge image, µfts appear in red, MTs in green and DNA in blue. Scale bar = 5µm. Quantif'Morphometric analysis of RORγt$^+$ and RORγt$^-$ iNKT cells (right panel): scatter dot plot analysis of cell size, nucleocytoplasmic ratio and cell circularity of RORγt$^+$ (triangles; n=82) and RORγt$^-$ (rounds; n=95) cells. For each parameter, mean value and standard deviation are presented as red bars ($_{****}$: P<0.0001, Mann-Whitney U test). Three independent experiments were analysed. Cell size was estimated in µm^2 using the Z-stack projections of actin staining. Similarly, nucleus size (µm^2) was estimated using DAPI Z-stack projections to calculate the nucleo-cytoplasmic ratio. Cell circularity indicative of cell shape and cell elongation was directly measured using Fiji software.

B. Granularity and size of thymic CD138$^+$ vs CD138$^-$ iNKT cells were analyzed by SSC-A (left) and FSC-A (right) in the thymus as shown in representative dot plots. Histograms show mean fluorescence intensity of SSC-A and FSC-A of the indicated subsets.

C. Representative histogram plots of Nrp-1 expression in thymic tet$^+$RORγt$^-$ and tet$^+$RORγt$^+$ iNKT cells from 6-wk-old B6-ROR*gfp*Tg mice. Histograms show the frequency of Nrp-1 expressed on thymic tet$^+$RORγt$^-$ or RORγt$^+$ iNKT at the indicated ages or on tet$^+$RORγt$^+$CCR6$^+$ or CCR6$^-$ iNKT cells.

D. Representative dot plots of intracellular nuclear BrdU staining of gated thymic tet$^+$RORγt$^+$ and tet$^+$RORγt$^-$ iNKT cells from 6-wk-old B6 mice after 2 wk of continuous exposure to BrdU in drinking water (left) then 2 weeks without BrdU (right). Histogram shows the frequency of BrdU$^+$ cells among the indicted subsets and timing of BrdU exposure.

Data from B, C, and D, are from 4 to 7 experiments with 3 to 5 mice used per experiment. Significance is represented by an asterisk and was evaluated with non-parametric Mann-Whitney U test. A *p* value <0.05 was considered significant. NS: non-significant. Numbers represent percentages of positive cells. Iso: isotype control. Ic: intracellular nuclear staining.
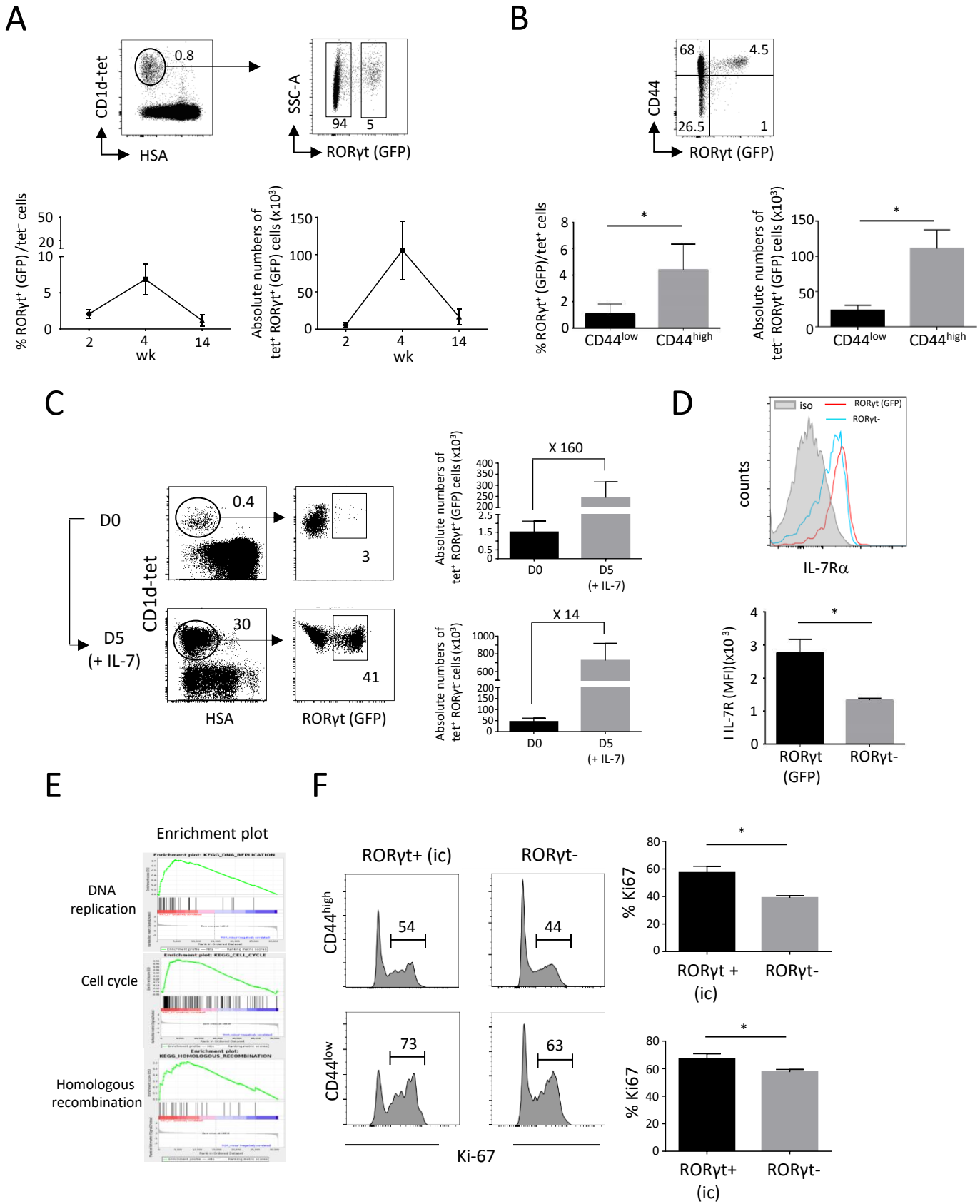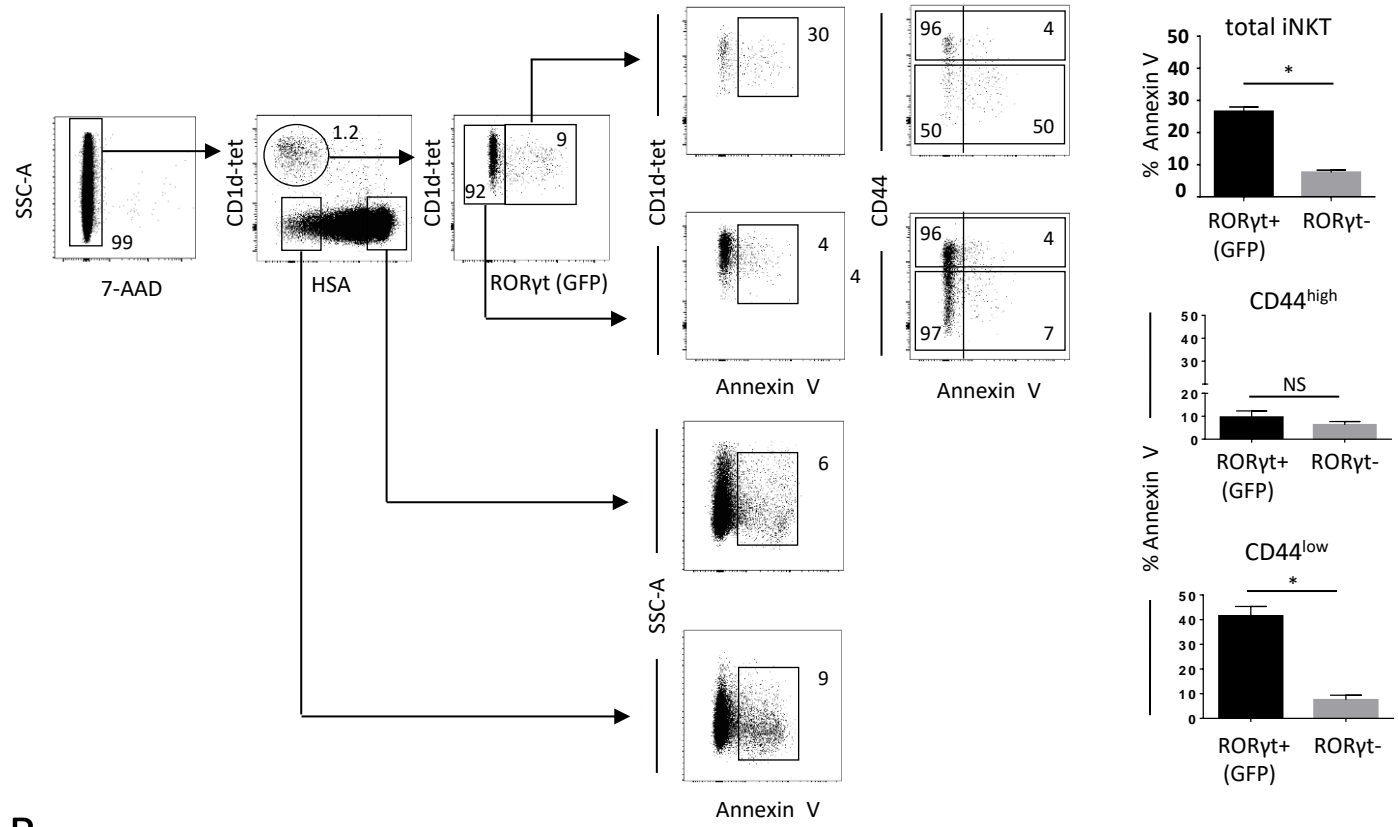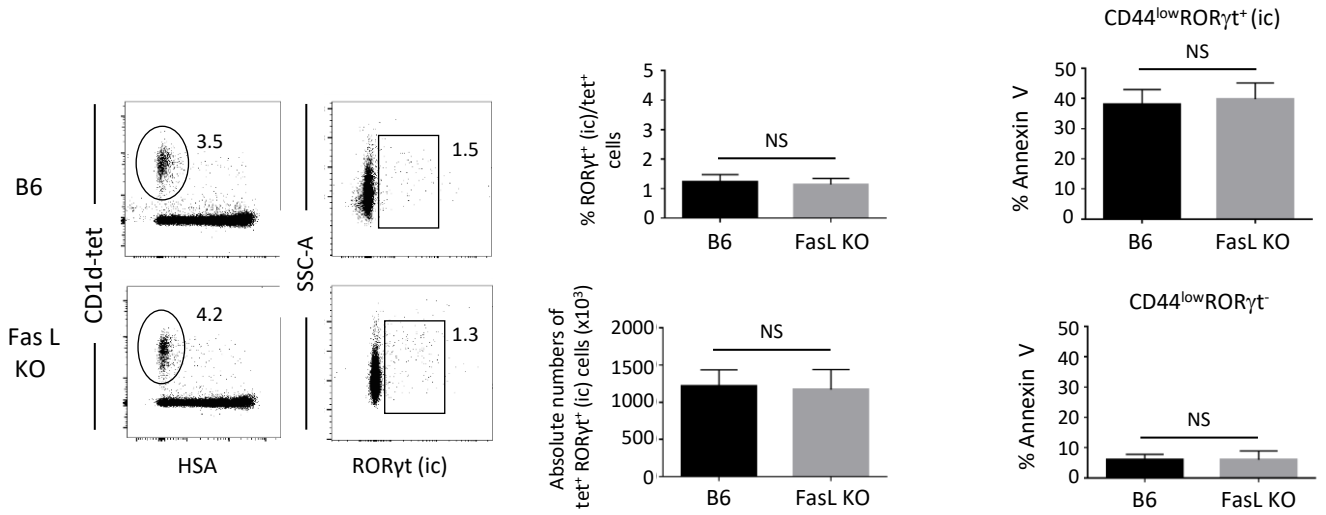
Figure 5: TCR signal strength assessed by CD5 expression <mark>AQ10</mark>

A. Representative Histograms plots of CD5 staining gated on total, CD44^{low} or CD44^{high} <mark>thymic</mark> iNKT1, 2, or 17 iNKT cell subsets from 2-wk-old B6 mice. Histograms show mean fluorescence intensity (MFI) of CD5 at the indicated <mark>subsets</mark>.

B. Representative dot plot of annexin V staining on total, CD44^{low} or CD44^{high} thymic iNKT1, 2, or 17 iNKT cell subsets from 2-wk-old B6 mice. Histograms represent the frequency of annexin V$^+$ cells at the indicated stages.

Data are from at 5 experiments where 4 to 6 mice were used per experiment. Significance is represented by an asterisk and was evaluated with non-parametric Mann-Whitney U test. A p value <0.05 was considered significant. <mark>NS: non-significant. Iso: isotype control. Numbers represent percentages of positive cells.</mark>

Figure 1

Figure 2

Figure 3

A

B

Gated on tet+RORγt+ (GFP)

C

CD44high

CD44high

CD44low

CD44low

D

RORγt (GFP)

MFI (RORγt (GFP))

E

%IL-17+/tet+RORγt+ (GFP)

F

tet+ CD44highRORγt+ (ic)
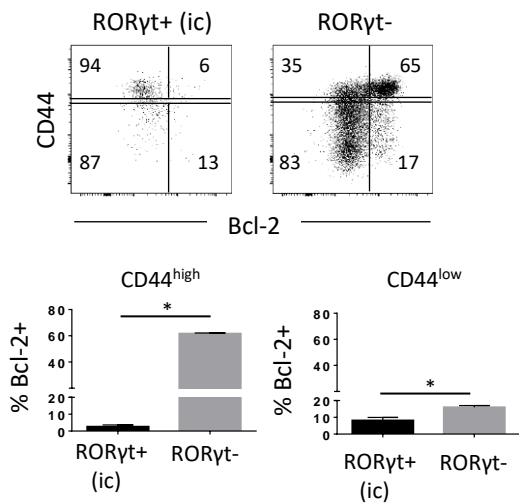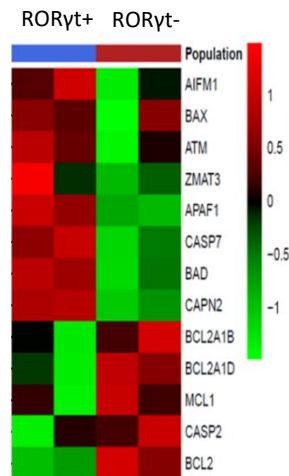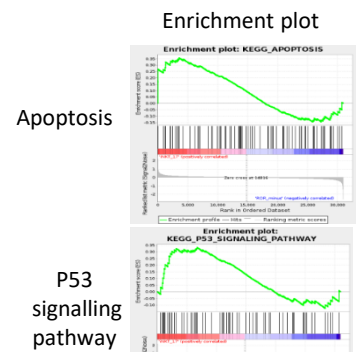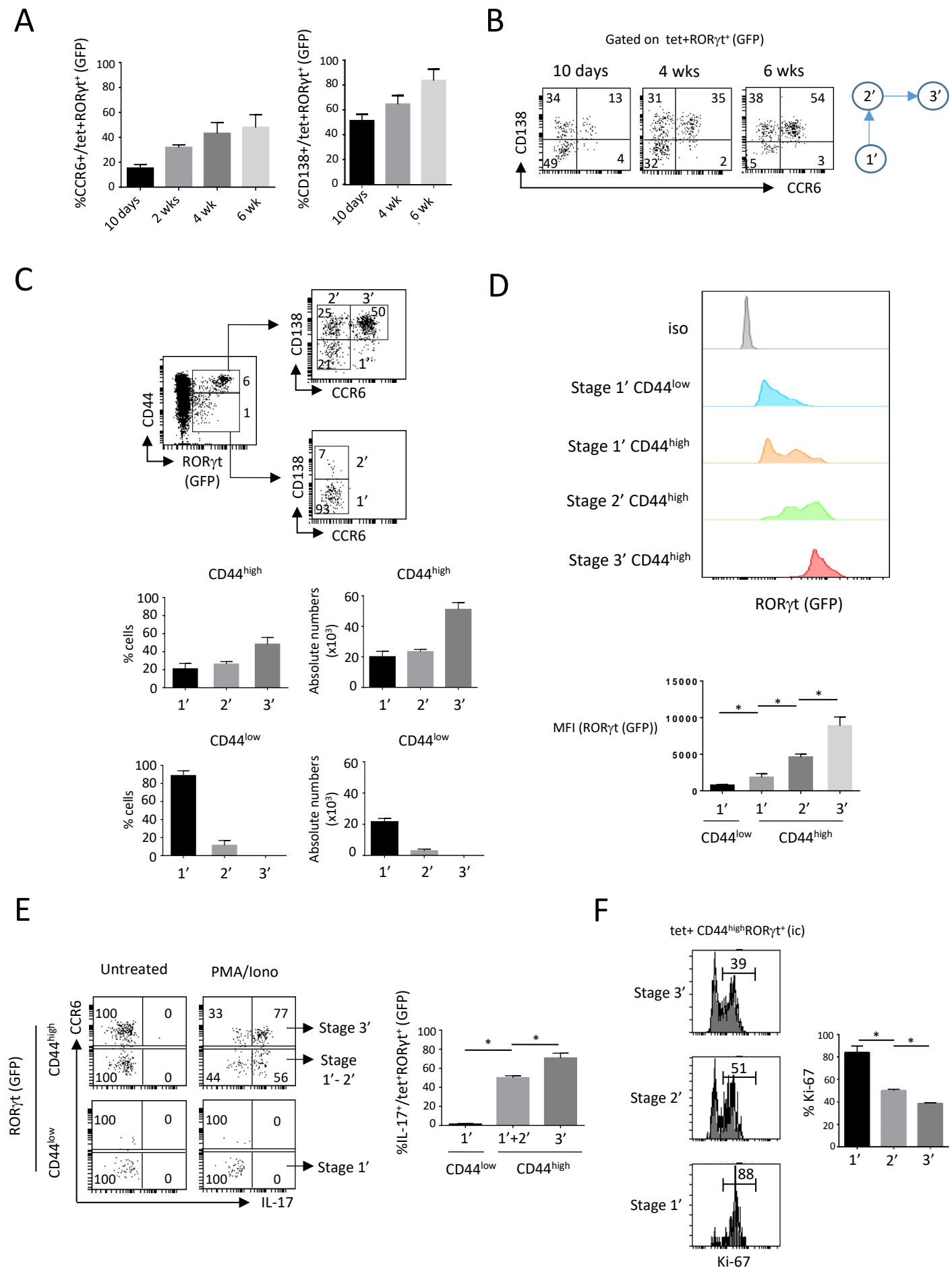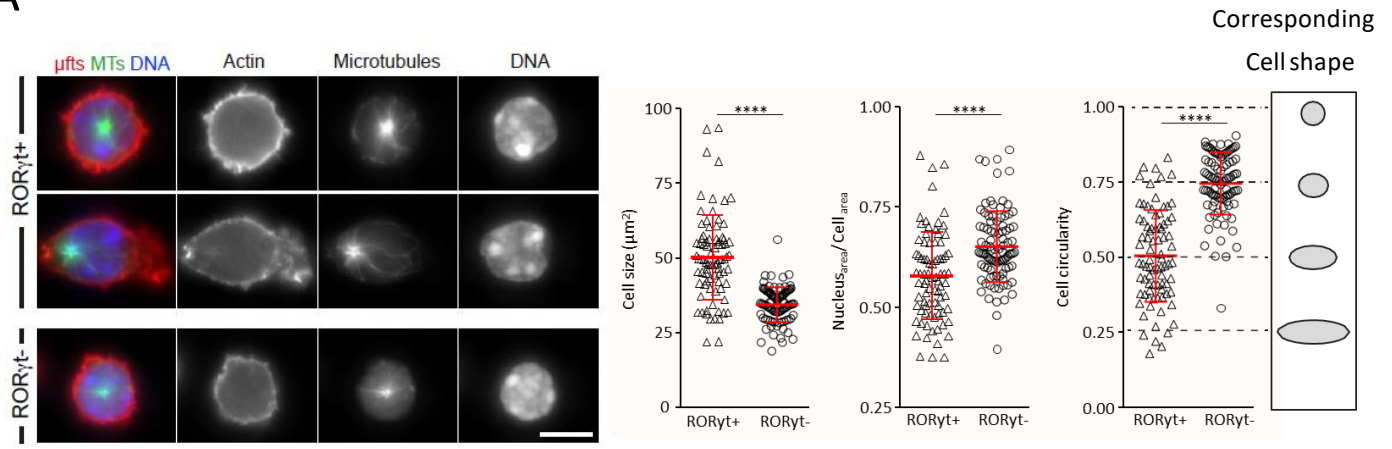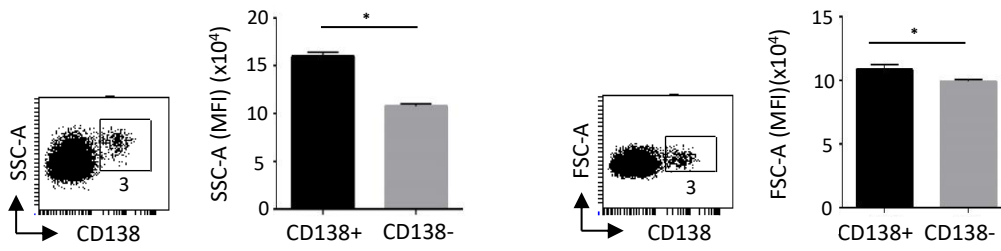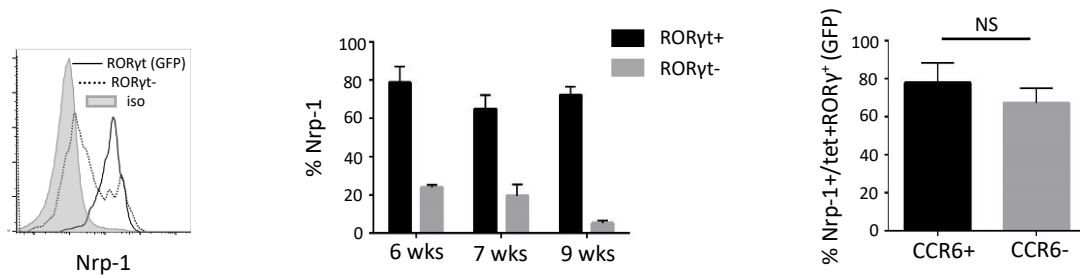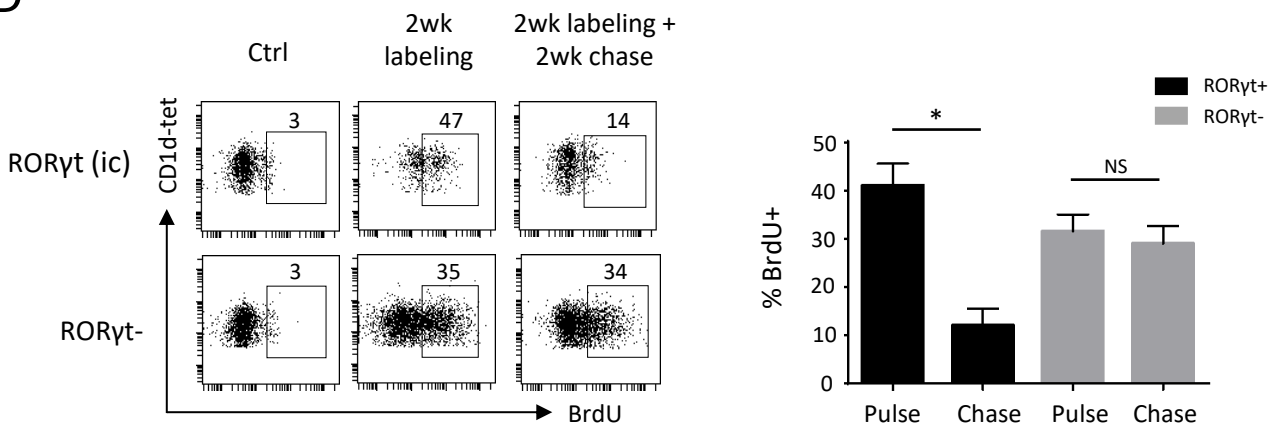
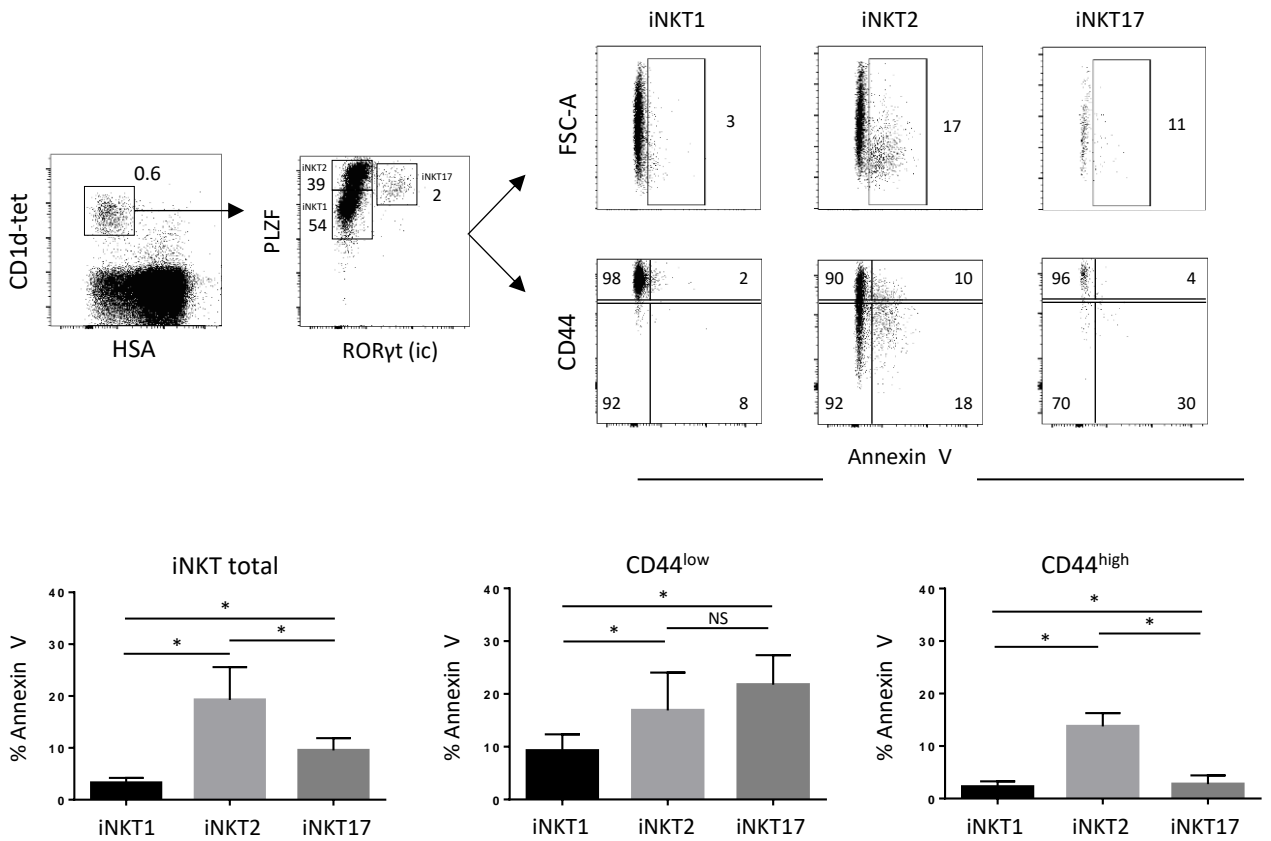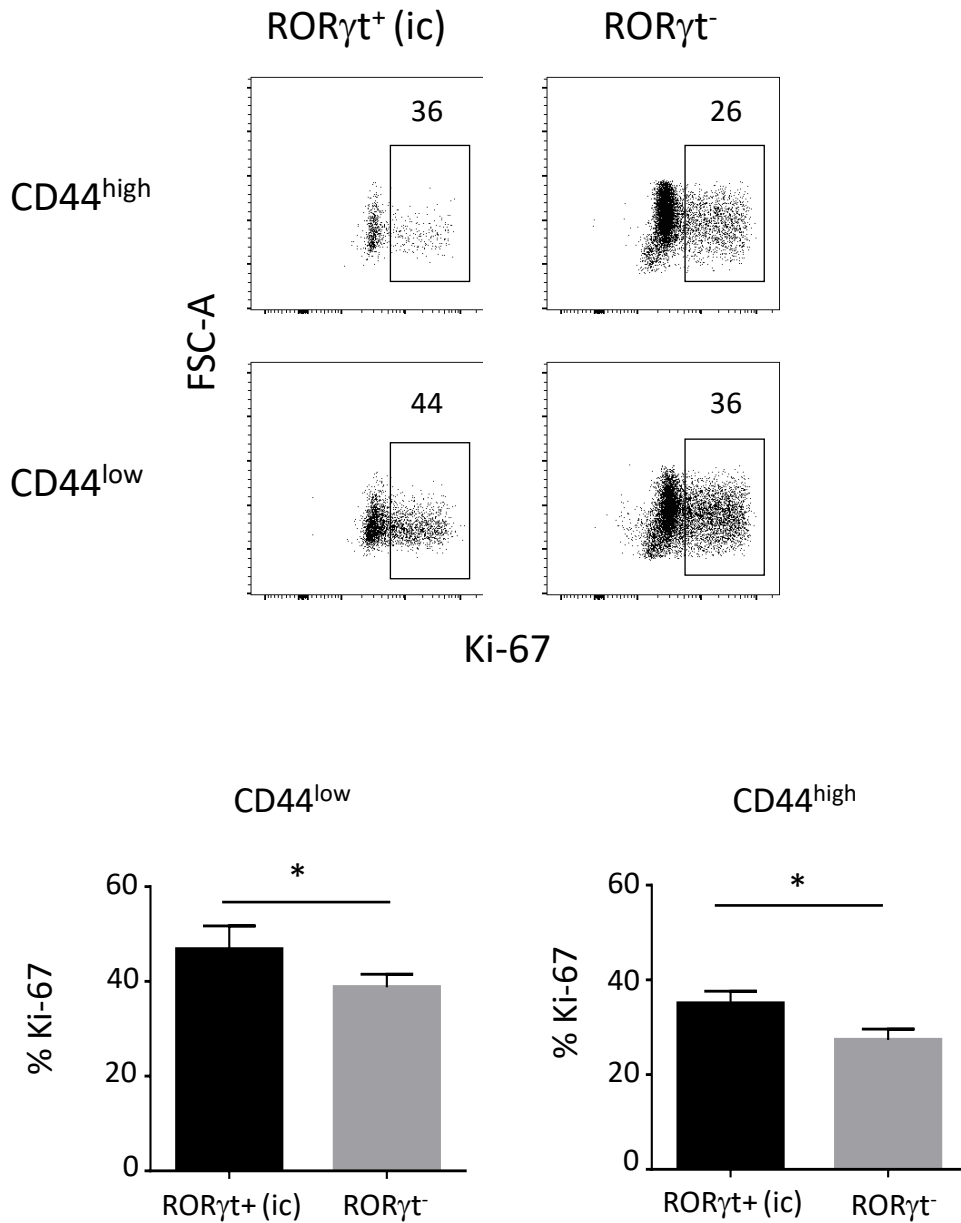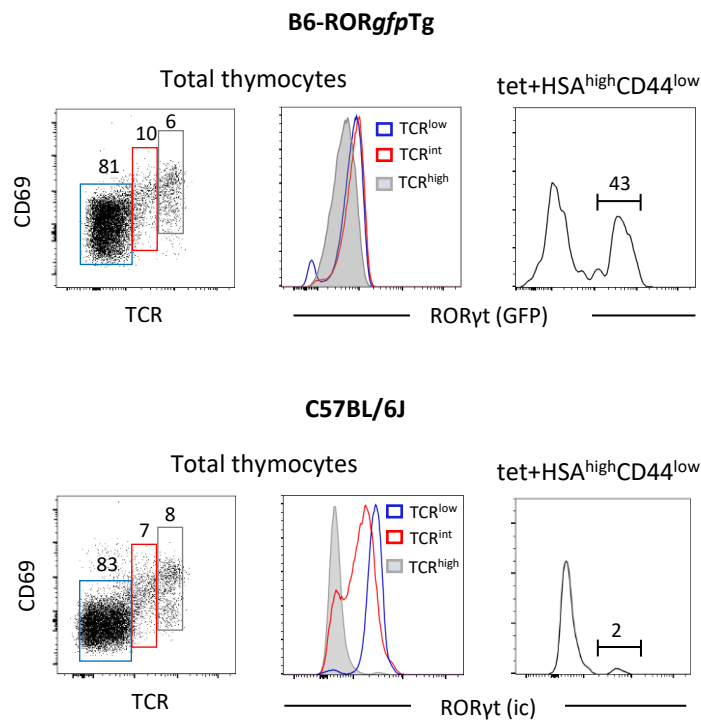
% Ki-67

Ki-67

Figure 4

Figure 5
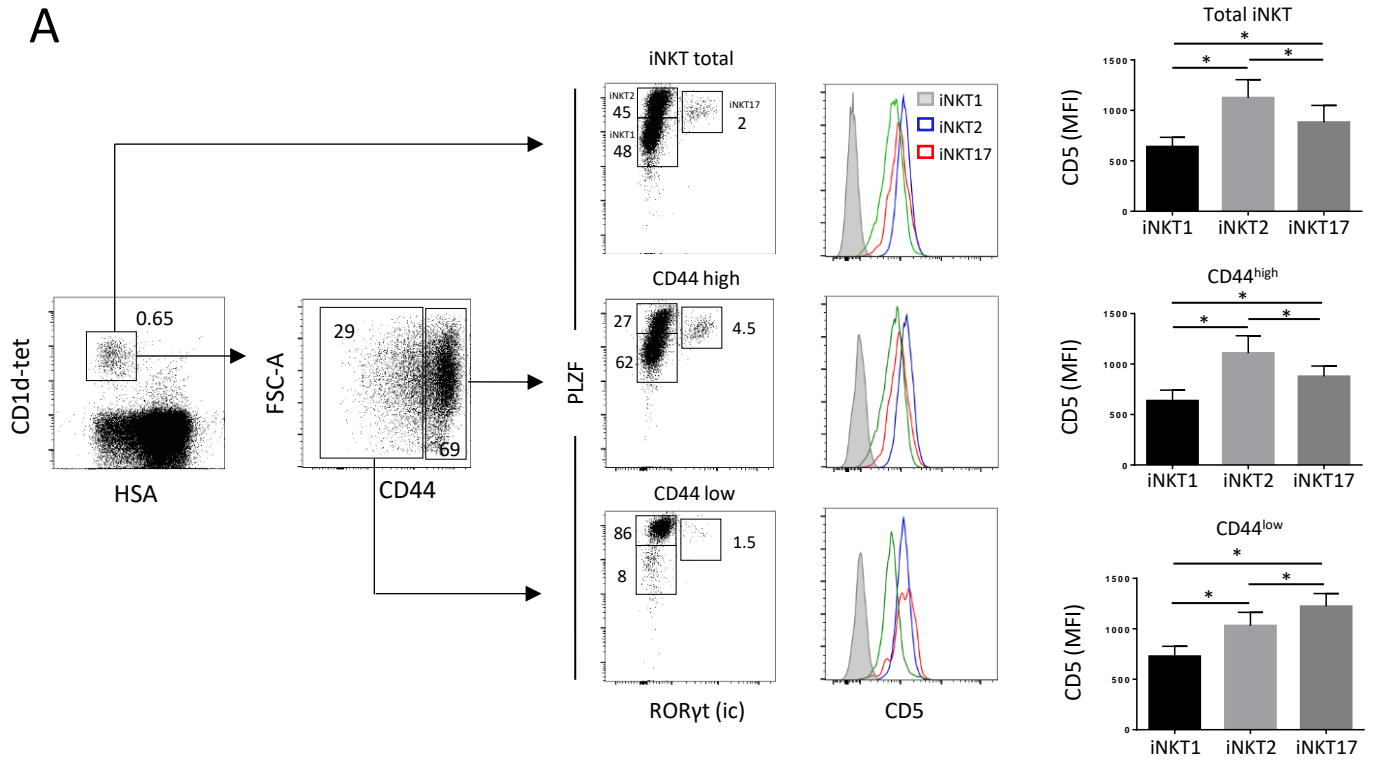
Fig. S1: RORγt+iNKT cells from BALB/c mice experience a greater proliferation than RORγt- iNKT cells.
Flow cytometry analysis of Ki-67+ cells in the thymus gated on tet+RORγt+ or RORγt- iNKT cells at the CD44low and CD44high stage of 6-wk-old BALB/c mice assessed by intracellular nuclear staining (ic) . Histograms show Ki67 frequencies in the indicated stages. Data are from 3 experiments where 3 to 4 mice were used per experiment. Numbers represent percentages. Significance is represented by an asterisk and was evaluated with non-parametricMann-Whitney U test. A *p* value <0.05 was considered significant. Ic: intracellular nuclear staining.

B6-ROR*gfp*Tg

Total thymocytes   tet+HSA^high^CD44^low^

C57BL/6J

Total thymocytes   tet+HSA^high^CD44^low^

Fig. S2: B6-ROR*gfp*Tg mice is not suitable to study HSA^high^ stage 0 iNKT cells
Upper panel: Flow cytometry analysis of RORγt expression gated on thymocytes differentially expressing TCR and CD69 as depicted and defining TCR^low^, TCR^int^, and TCR^high^ thymocytes (left dot plot and middle histogram plot) and in HSA^high^ CD44^low^ iNKT cells (far right histogram plot) obtained from 2-4-wk-old B6-ROR*gfp*Tg mice. Lower panel: Flow cytometry analysis of RORγt expression, assessed by intracellular nuclear staining (ic), in TCR^low^, TCR^int^, and TCR^high^ thymocytes (left dot plot and middle histogram plot) and in HSA^high^ CD44^low^ iNKT cells (far right histogram plot) obtained from 2-4-wk-old B6 mice.
Data are from at least 5 experiments with three mice used per experiment. iNKT cells are enriched by magnetic beads like described previously (ref#2) and assessed for Vβ8 bias to ensure they are bona fide iNKT cells. Numbers represent percentages of cells at the indicated subsets. Ic: intracellular nuclear staining.
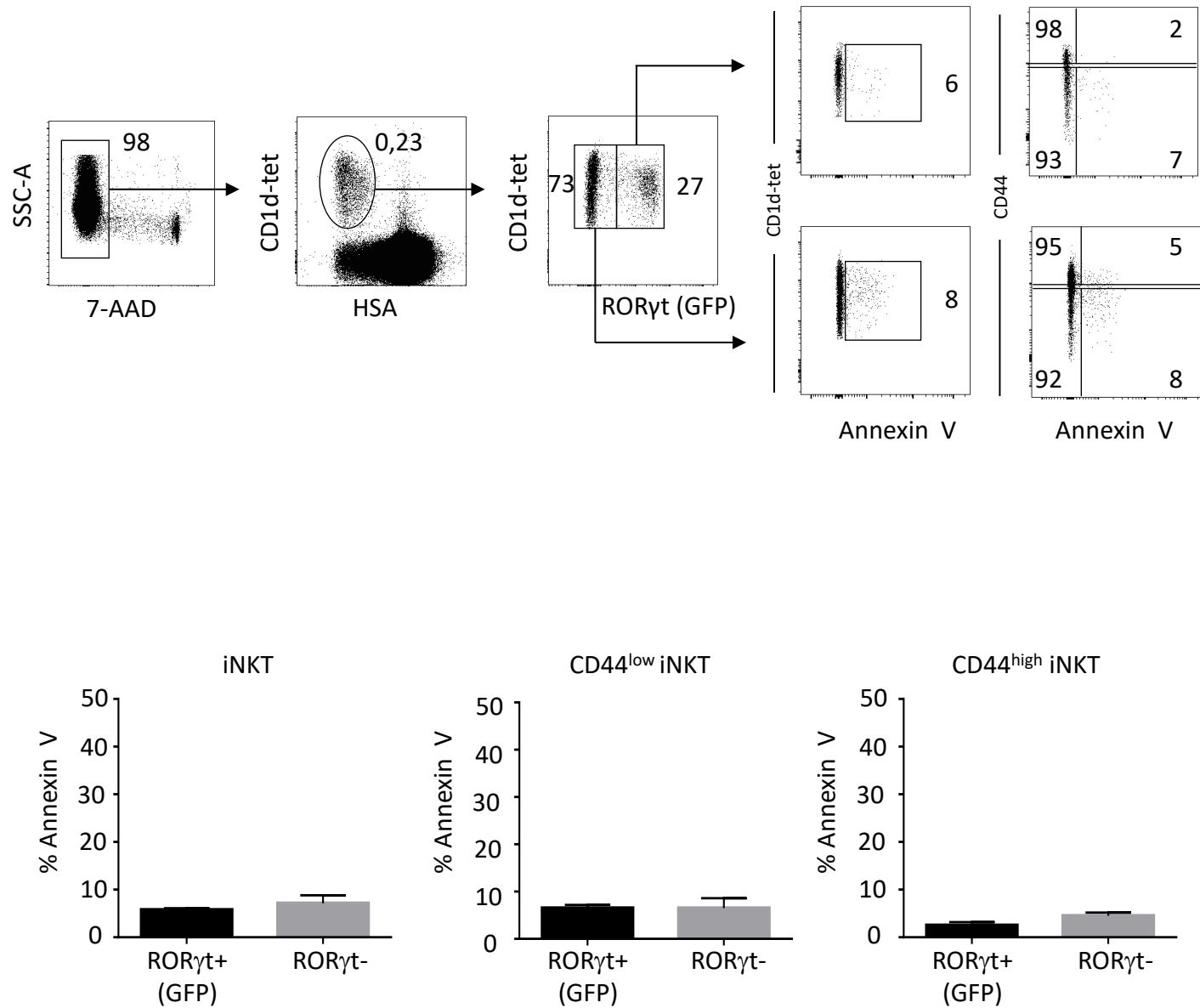
Fig. S3: RORγt+iNKT cells from BALB/c mice do not experience apoptosis during their development
Thymic RORγt+ vs RORγt- iNKT cells at the CD44low or CD44high stage from 6-wk-old BALB/c- ROR*gfp*Tg mice are analyzed by flow cytometry for apoptosis after Annexin V and 7-AAD staining. Histograms represent the frequency of annexin V+ cells in the indicated stages. Numbers represent percentages of positive cells in the indicated gates. Data are from 3 experiments where at least 3 mice were used per experiment.
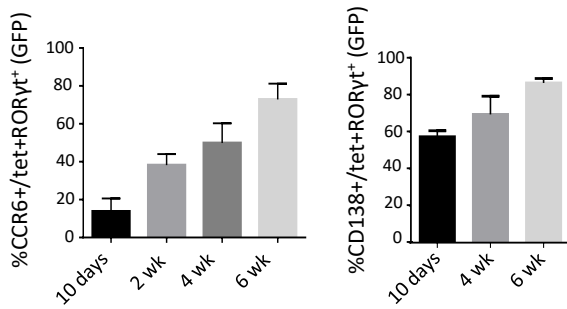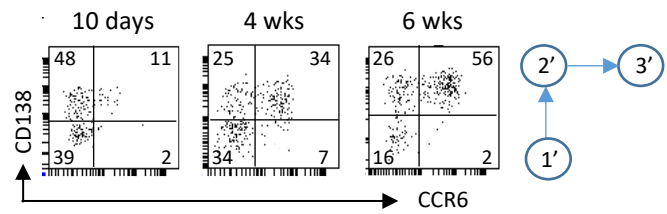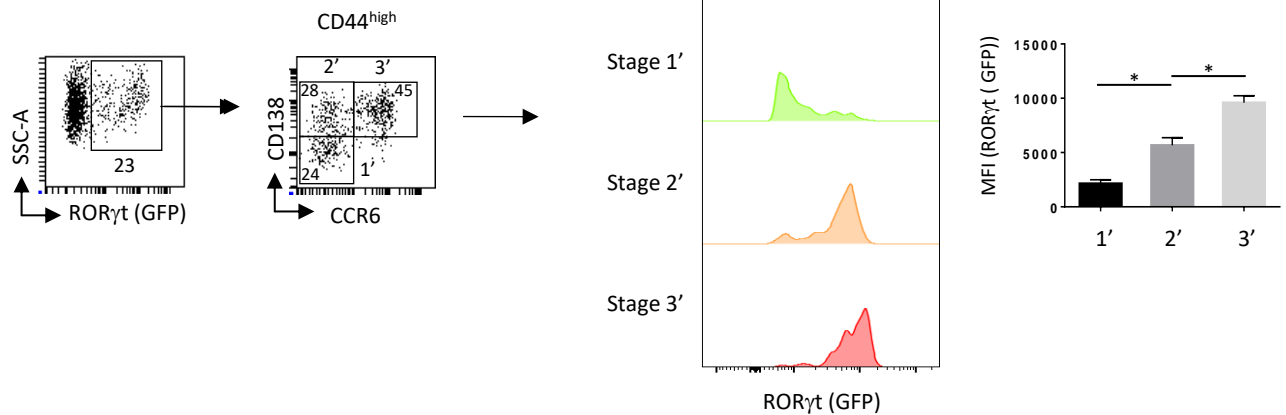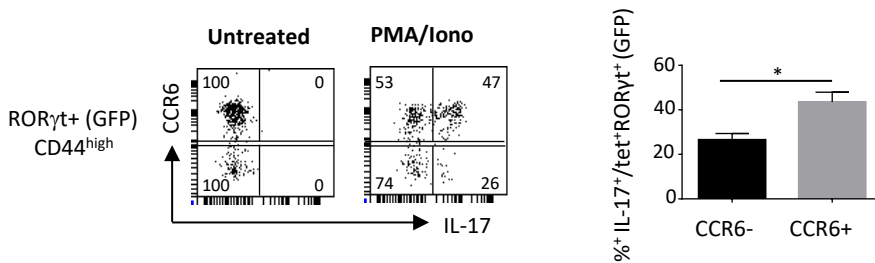
Fig. S4: Ontogeny of RORγt⁺ iNKT cells in PLNs

A. Histograms show the frequencies of CCR6 and CD138 positive cells among tet⁺RORγt⁺ iNKT cells in PLNs from B6-ROR*gfp*Tg mice at the indicated ages.

B. Representative dot plots of CD138/CCR6 expression among tet⁺RORγt⁺CD44^high iNKT cells in PLNs from B6-ROR*gfp*Tg mice at 10 days, 4 wk, and 6 wk of age.

C. Representative histogram plots of RORγt⁺ expression at the indicated stages, among tet⁺RORγt⁺ CD44^high iNKT cells from 4-wk-old ROR*gfp*Tg mice. Histograms show the frequencies of RORγt⁺ expression at the indicated stages.

D. Representative histogram plots of IL-17a gated on PLN CCR6⁻ or CCR6⁺tet⁺CD44^highRORγt⁺iNKT from 6-wk-old B6-ROR*gfp*Tg mice analyzed after 4h PMA/Ionomycin stimulation. Histograms show the frequencies of IL-17a positive cells among the indicated RORγt⁺ iNKT cell subsets.

Data are from 5 to 7 experiments where 3 mice were used per experiment. Numbers represent percentages of positive cells. Significance is represented by an asterisk and was evaluated with non-parametric Mann-Whitney U test. A *p* value <0.05 was considered significant. MFI: mean fluorescence intensity. Iso: isotype control.
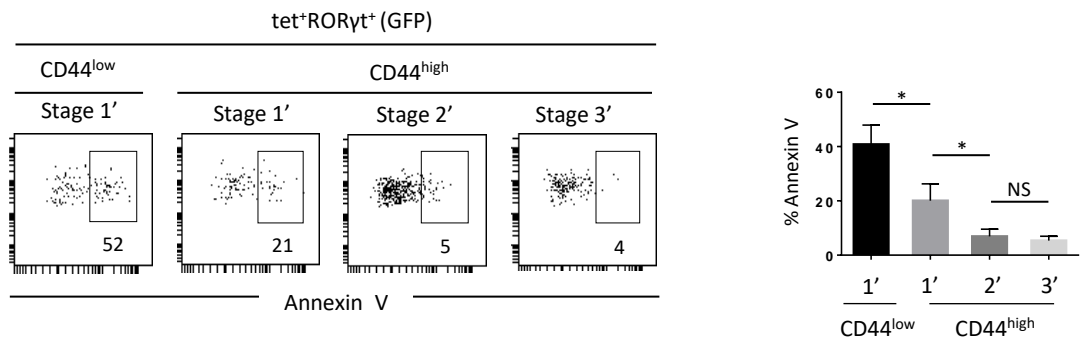
Fig. S5: **Progressive reduction in the propensity to apoptosis of RORγt⁺ iNKT**

Representative histogram plots of annexin V expression among thymic tet⁺RORγt⁺ CD44^{low} or CD44^{high} iNKT cells from 4-wk-old B6-ROR*gfp*Tg mice. Histograms show the frequencies of annexin V and RORγt expression at the indicated stages among tet⁺RORγt⁺CD44^{high} or CD44^{low} iNKT cells.

Data are from 4 to 6 experiments where at least 3 mice were used per experiment. Significance is represented by an asterisk and was evaluated with non-parametric Mann-Whitney U test. A *p* value <0.05 was considered significant. NS: non-significant. Numbers represent percentages of positive cells in the indicated gates.
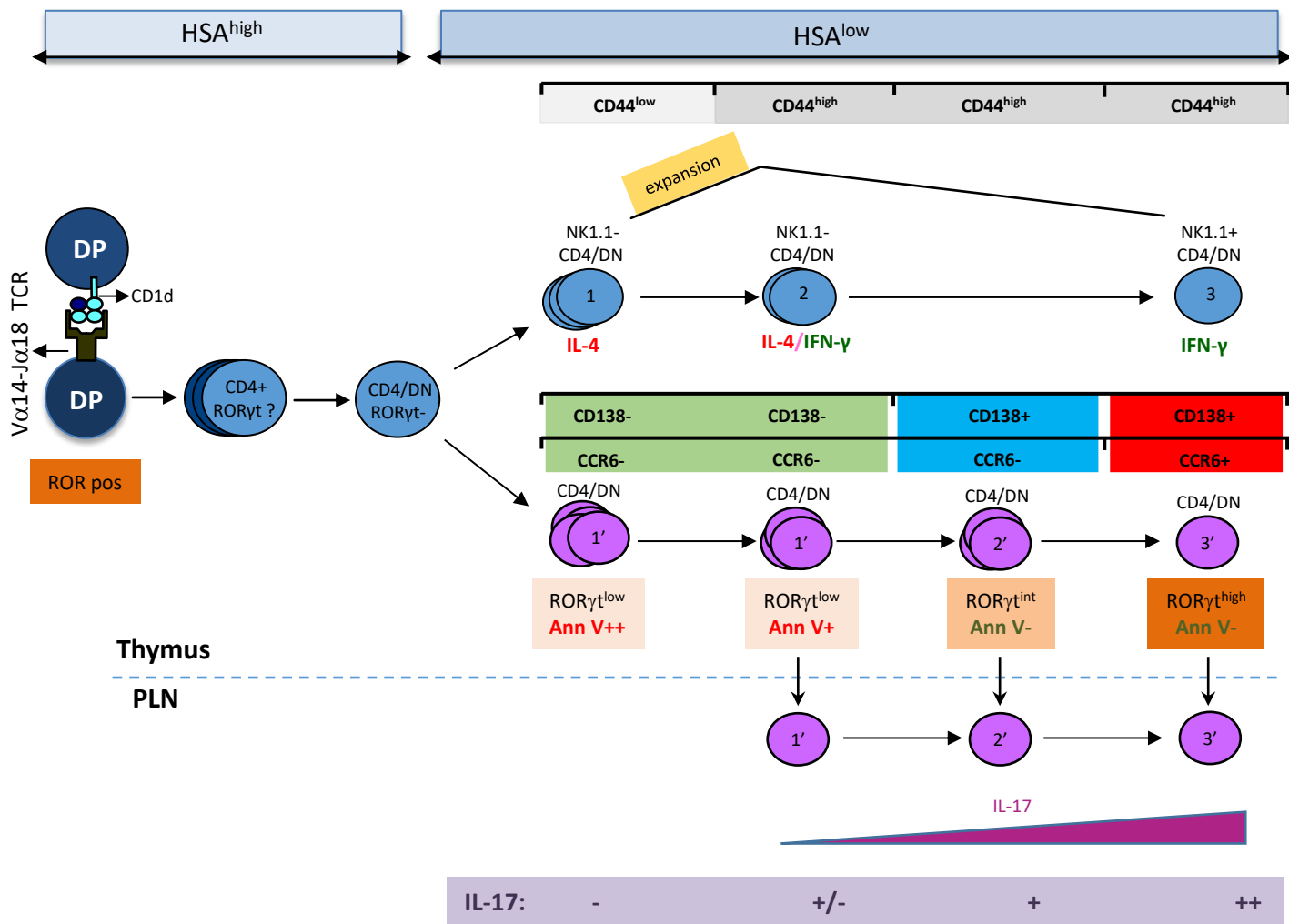
Suppl. figure 6

Fig. S6: proposed model of thymic and peripheral RORγt⁺ iNKT cell development based on the analysis of B6-ROR*gfp*Tg mice

The earliest iNKT cell precursors we are able to detect are HSA^{high} stage 0 iNKT cells. At the subsequent HSA^{low}CD44^{low} stage, RORγt⁺ iNKT17 cells perceive a strong TCR signal compared to RORγt⁻ iNKT1 cells. Both subsets undergo a massive expansion, with a higher expansion observed for RORγt⁺ iNKT cells, accompanied with a greater susceptibility to apoptosis. At this stage RORγt⁺ iNKT do not express CCR6 or CD138 (this stage is called stage 1' at the CD44^{low} stage). At the potential following CD44^{high} stage, CD138 and CCR6 are progressively acquired and cells likely progress from stage 1' (CCR6⁻CD138⁻) to stage 2' (CCR6⁻CD138⁺) and ultimately to stage 3' (CCR6⁺CD138⁺). Ontogeny studies in the thymus and PLNs combined with BrdU labeling suggested that RORγt⁺ iNKT cells might not reside in the thymus and that maturation of RORγt⁺ iNKT cells could take place in the thymus and PLNs. It is important to mention that this is a speculative model and direct evidences are needed to prove it.